Experimental Hematology & Oncology

RESEARCH

Open Access

ELK1 promotes the progress of myeloid leukemia by hindering the differentiation of neutrophils

Yuhan He[1†], Ya Zhou[2†], Dexin Wen[1†], Rongqun Guo[3], Juan Du[4], Sizhou Huang[5] and Yong Dong[1,2*]

Abstract

Background The genes controlling lineage determination and differentiation tend to be essential for the development of acute myeloid leukemia (AML). Identifying novel target genes capable of promoting the differentiation and maturation of undifferentiated leukemia cells offers a promising therapeutic strategy for the treatment of AML.

Methods We used conditional Elk1 and KrasG12D expression mice, along with Mx1-Cre, Lyz2-Cre and Elane-Cre drive strains (which enable stage specific control of Elk1 or KrasG12D expression), to investigate the function of Elk1 in the hematopoiesis and leukemogenesis. Bone marrow transplantation assay was performed to explore the function of Elk1 in hematopoiesis under stress conditions. Additionally, bulk-cell RNA sequencing, single-cell RNA sequencing and proteomics were performed to reveal the signaling pathways altered by Elk1. Finally, undifferentiated leukemia cells were used to verify whether inhibiting ELK1 could promote the differentiation of these cells into mature neutrophils.

Results ELK1 is highly expressed in undifferentiated AML cells. Studies using mouse model demonstrated that overexpression of Elk1 accelerates the development of KrasG12D-induced myeloid leukemia by impairing the stemness of hematopoietic stem cells (HSCs) and impeding the differentiation of neutrophils. Furthermore, impeding the maturation of neutrophils independently promotes the development of KrasG12D mutation-induced myeloid leukemia. Meanwhile, our in vitro experiments preliminarily confirmed that inhibiting ELK1 suppresses the proliferation of leukemia cells and induces the differentiation of $CD15^{+}CD66b^{-}$ myeloid progenitor cells into $CD15^{+}CD66b^{+}$ neutrophils.

Conclusions Our study demonstrates that ELK1 is a potential therapeutic target for AML, due to its critical role in regulating neutrophils differentiation.

†Yuhan He, Ya Zhou and Dexin Wen contributed equally to this work.

*Correspondence:
Yong Dong
dongyong@cmc.edu.cn

Full list of author information is available at the end of the article

Highlights

1. Human ELK1 is highly expressed in AML undifferentiated cells and negatively correlated with the survival of AML patients.
2. Upregulation of Elk1 impairs the self-renewal of HSCs, impedes the differentiation of neutrophils under physiological conditions and promotes the development of oncogene mutation (KrasG12D)-induced myeloid leukemia.
3. Under stress hematopoiesis conditions, upregulation of Elk1 promotes the depletion of neutrophils.
4. Elk1 promotes the development of oncogene mutation (KrasG12D)-induced myeloid leukemia by impeding the maturation of neutrophils.

Keywords ELK1, Neutrophil depletion, Hematopoiesis, Leukemogenesis, Myeloid leukemia

Introduction

Acute myeloid leukemia (AML) is characterized by the accumulation of undifferentiated myeloid progenitors. Promoting the differentiation of undifferentiated leukemia cells into functional mature cells is one of the strategies to treat AML. Currently, drugs like daunorubicin, cytarabine, idarubicin, mitoxantrone, venetoclax and clofarabine are commonly used in AML treatment. These medications primarily function by inhibiting clonal proliferation of lineage progenitor cells or inducing apoptosis, rather than promoting the differentiation and maturation of leukemia cells. However, when used independently, the 5-year survival rate of AML patients treated with these drugs is less than 50% [1]. In contrast, the treatment of APL with trans-retinoic acid and trioxide has achieved remarkable success, with an event - free survival rate exceeding 97%. This success is attributed to the drugs' ability to promote the differentiation and maturation of immature neutrophils [2] .

To find methods for promoting the differentiation of undifferentiated leukemia cells, we need to focus on lineage differentiation regulator genes. At present, multiple lineage differentiation key regulator genes are reported to play critical role in leukemia development. Such as GFI1 [3], CEBPA [4], CEBPE [5] and IRF8 [6], which regulate the myeloid lineage differentiation and maturation, have been identified as risk factor for AML [7–9]. However, targeting these risk factors in AML therapy has not yielded the expected efficacy due to their complex roles in hematopoiesis. For instance, knocking down GFI1 [10]and CEBPA [11] impairs the self-renew of HSC and normal hematopoiesis, and mutation of CEBPE leads to the granule deficiency in neutrophils [12]. The scarcity of highly specific targets in regulating the lineage differentiation and maturation limits the application of new approaches to treat AML by promoting the differentiation and maturation. Therefore, there is an urgent need to screen lineage specific regulators as new targets to treat AML.

RAS genes are frequently mutated in leukemia. The mutated RAS genes activate the downstream MEK/ERK axis to disrupt the differentiation of hematopoietic stem/progenitor cells [13, 14]. Although the ERK-ELK1 signal is reported to regulate cell differentiation [15, 16] and promote the development of solid tumor [17, 18], differential roles of RAS and ELK1 in hematopoietic lineage differentiation have been documented. For example, knockout of K-Ras significantly reduced the number of erythroid progenitors and mature erythrocytes [19], while upregulation of ELK1 significantly hinders the differentiation of erythroid progenitors [20]. RAS promotes the differentiation of neutrophils by activating C/EBPα [21], but not by activating ELK1. However, upregulation of ELK1 blocks the differentiation of neutrophils [20, 22]. The inconsistence function of RAS and ELK1 might be due to the complex regulation of ELK1, which regulates the differentiation and proliferation in multiple ways, including RNA splicing [22], phosphorylation self-limitation [23], protein cleavage [24]. Additionally, our previous research has shown that ELK1 plays a crucial regulatory role in the differentiation and maturation of human neutrophils and balancing lineage determination of neutrophils and erythrocytes at the CMP stage under ex vivo culture conditions [20, 22]. Thus, we suspect that ELK1 might play an important role in the development of myeloid leukemia, and targeting ELK1 might promote the differentiation of undifferentiated leukemia cells into mature cells. In this study, we intensively investigated the in vivo functions of Elk1 in hematopoiesis and leukemogenesis by using Elk1 and KrasG12D conditional expression mouse models.

Materials and methods

Mice

C57BL/6 (CD45.1^{+}) and KrasG12D$^{LSL/+}$ (Kras$^{loxp-stop-loxp-G12D/+}$)mice were purchased from Shanghai Model Organisms Center, Inc. Mx1-Cre (C57BL/6, CD45.2+) was purchased from Cyagen Biosciences, Inc. *Elane*-Cre (C57BL/6, CD45.2+) and *Lyz2*-Cre (C57BL/6, CD45.2+) mice were purchased from Labbio Biotechnology Co., Ltd. Elk1$^{LSL/+}$ (ROSA26$^{loxp-stop-loxp-Elk1-2a-tdTomato/+}$)mice were generated by

direct targeting the zygotes of C57BL/6 mice through CRISPR-Cas9 at the ROSA26 locus by Shanghai Model Organisms Center, Inc. as previously reported [18]. The expression of tdTomato was detected by flow cytometry analysis, which indicates the expression of Elk1, and it is more easy to distinguish donor derived cells in recipients. $Elk1^{LSL/+}$ mice were subsequently bred with Mx1-Cre, Elane-Cre and Lyz2-Cre mice to generate $Elk1^{LSL/+}$;Mx1-Cre, $Elk1^{LSL/+}$;Elane-Cre and $Elk1^{LSL/+}$;Lyz2-Cre mice. To assay the impact of Elk1 overexpression in KrasG12D-induced leukemia, $Elk1^{LSL/+}$;Mx1-Cre and $Elk1^{LSL/+}$;Elane-Cre were bred with $KrasG12D^{LSL/+}$ mice to generate $KrasG12D^{LSL/+}$-$Elk1^{LSL/+}$-Mx1-Cre, $KrasG12D^{LSL/+}$-$Elk1^{LSL/+}$-Elane-Cre, $KrasG12D^{LSL/+}$-Mx1-Cre and $KrasG12D^{LSL/+}$-Elane-Cre mice. All the mice were housed in SPF-grade (specific pathogen-free grade) animal facilities of Chengdu Medical College. All animal experiments were approved by the Institutional Animal Care and Use Committee of Chengdu Medical College (IACUC-CMC).

Transplantation

All recipient mice were irradiated for 5.0*2 Gy with RadSource 2000. All the recipient mice were anesthetized by a mixture of oxygen and isoflurane using the Matrx VMR small animal anesthesia machine before transplantation. For competitive transplantation, 0.5×10^6 total BM of $Elk1^{LSL/+}$-Mx1-Cre and 0.5×10^6 total bone marrow (BM) cells of C57BL/6 (CD45.1+) were retro-orbitally transplanted into lethally irradiated C57BL/6 (CD45.2+) recipients (5.0 Gy x2, RS2000, Rad Source). For non-competitive transplantation, 1.0×10^6 total BM of donor cells ($Elk1^{LSL/+}$-Mx1-Cre, $Elk1^{LSL/+}$-Elane-Cre, $Elk1^{LSL/+}$-Lyz2-Cre $KrasG12D^{LSL/+}$-$Elk1^{LSL/+}$-Mx1-Cre, $KrasG12D^{LSL/+}$-$Elk1^{LSL/+}$-Elane-Cre, $KrasG12D^{LSL/+}$-Mx1-Cre, $KrasG12D^{LSL/+}$-Elane-Cre and littermate mice) were retro-orbitally transplanted into lethal irradiated recipients (CD45.2 or CD45.1 mice) anesthetized by the mixture of oxygen and isoflurane using the Matrx VMR Small Animal Anesthesia Machine. For the $Elk1^{LSL/+}$-Mx1-Cre, $Elk1^{LSL/+}$-$KrasG12D^{LSL/+}$-Mx1-Cre and $KrasG12D^{LSL/+}$-Mx1-Cre transplanted recipients, 200 μg Polyinosinic–polycytidylic acid sodium salt (PolyIC) (Sigma, P1530-100MG) was injected with 3 doses into all the recipients via intraperitoneal injection every other day. All transplanted mice were fed with water containing gentamycin sulfate to prevent infection for 3 weeks. Peripheral blood was collected from recipients using anticoagulant-coated capillary tubes via retro-orbital puncture every 4 weeks for flow cytometric analysis until 20 weeks post transplantation.

Flow cytometry analysis

Antibodies to CD45.1 (A20), CD45.2 (104), Ly6C (HK1.4), Ly6G (1A8), CD11B (M1/70), CD19 (6D5), B220 (RA3-6B2), CD4 (GK1.5), CD8a (53 – 6.7), Ter119 (TER-119), CD2 (RM2-5), CD3e (145-2c11), Ly6G/Ly6C (RB6-8C5), NK1.1 (S17016D), CD48 (HM48-1), CD150 (TC15-12F12.2), CD117 (2B8), Ly6A/E (Sca1, D7), CD25 (PC61), CD44 (IM7), CD16/32 (93), CD34 (HM34), CD135 (A2F10), CD115 (CSF-1R), CD81 (Eat-2), CD71 (RI7217), CD127 (A7R34), TCR γ/δ (GL3), TCR β (H57-597), IgM (RMM-1), IgD (11-26c.2a), CD184 (L276F12), CD284 (SA15-21), CD62L (MEL-14), CD182 (SA044G4) were purchased from BioLegend. 7-AAD was used for dead cells exclusion. Flow cytometry was performed on Canto II (BD Biosciences) and C6 plus (BD Biosciences) and data were processed by FlowJo software (Tree Star).

To analyze hematopoietic lineages and progenitors in PB or BM, CD3-FITC was used to stain T cells, CD19-APC was used to stain B cells, CD11b-PE-Cy7, Ly6G-FITC and Ly6C-APC were used to stain immature neutrophils, mature neutrophils and monocytes, CD71 and Ter119 were used to stain erythrocytes, and the antibody mixture of Lin (CD2, CD3, CD4, CD8, CD11b, Gr1, Ter119, B220)-FITC, CD48-FITC, c-Kit (CD117)-APC, Sca1-PerCP-Cy5.5, CD150-PE-Cy7 were used to analyze Lin-CD48-c-$Kit^+Sca1^+CD150^+$ HSC(hematopoietic stem cell) and Lin-CD48-c-$Kit^+Sca1^+CD150^-$ MPP(multipotent progenitor), Lin (CD2, CD3, CD4, CD8, CD11b, Gr1, Ter119, B220)-FITC, c-Kit (CD117)-APC, CD16/32-PE-Cy7, Sca1-PerCP-Cy5.5, CD34-APC-Cy7 were used to analyze Lin^- $c\text{-}Kit^+$ $Sca1^-CD16/32^{mid}$ $CD34^{mid}$ CMP (common myeloid progenitor), Lin^- $c\text{-}Kit^+$ $Sca1^-$ $CD16/32^{high}$ $CD34^{high}$ GMP(granulocyte-monocyte progenitor) and Lin^- $c\text{-}Kit^+$ $Sca1^-$ $CD16/32^-$ $CD34^-$ MEP (megakaryocyte–erythroid progenitor).

RNA sequencing and data analysis

To assess the transcriptome of LSKs, CMPs, GMPs, MEPs and mature neutrophils, 3000 cells of each population were sorted and collected with PCR tubes with 0.5%BSA-PBS buffer, and cell pellet was harvested by removing the supernatant liquid after centrifuging at 500 g for 5 min. All transcripts were converted into dsDNA for each population according to previously reported procedures [22, 25–27]. Libraries were constructed using TruePrep DNA Library Prep Kit V2 for Illumina (TD503, Vazyme, Co.Ltd) and all the libraries were sequenced using the Illumina NovaSeq X plus system (HaploX company. Ltd.). R packages DESeq2, gplots, clusterProfiler and GSEA were used to analyze the differential expressed genes (DEGs), GO enrichment and gene set enrichment analysis (GSEA).

To analyze the myeloid differentiation pathway at single-cell level, CD3/CD19/NK1.1/$Ter119^-$ $CD11b^+$ and

CD3/CD19/NK1.1/Ter119/C-kit$^+$ cells derived from Mx1-Elk1 and littermate control mice were sorted and these two cell populations were mixed at a ratio of 1:2 and processed using the 10X Genomics Chromium system, then single cell libraries generation and sequencing were performed by NovaSeq 6000 system (library construction and sequencing of single cell were performed by HaploX Company). All FASTQ files were mapped to mouse mm10 reference genome to generate gene expression matrices by Cell Ranger 4.0.4 software. The R packages including Seurat, clusterProfiler, ggplot2 were used to analyze the single cell RNAseq data. The R package ClusterProfiler was used to analyze GO enrichment for DEGs.

Proteomics assay

Bone marrow cells were isolated from femurs and tibias of 8-weeks-old Elane-Elk1 and littermate mice. For each sample, 3×10^4 CD11b$^+$ Ly6G$^{low/-}$Ly6C^{mid} immature neutrophils or CD11b$^+$ Ly6G$^+$ Ly6C^{mid} mature neutrophils were sorted for proteomic assay. The proteomic assay of the sorted cells was performed by Shanghai Bioprofile Company. Differentially expressed proteins (DEPs) were identified with the threshold of 1.5-fold change and p-value < 0.05. The function of differentially expressed proteins was analyzed by clusterProfiler and gplots R packages.

AML leukemia cells culture

OCI- AML 3 (CL-0837) was kindly provided by Wuhan Pricella Biotechnology Co.,Ltd, HL-60, Molm-13, NB4 and Kasumi-1 cell lines were gifts from Yuhuan Zheng's Lab (Department of Hematology/Institute of Hematology, West China Hospital, Sichuan University). The OCI-AML3 cell line harbors NPM1 and DNMT3A gene mutations. The Molm-13 cell line carries an FLT3 gene mutation. The NB4 cell line expresses the PML-RARα fusion genes, which results from the t (15;17) translocation. The Kasumi-1 cell line carries the AML1-ETO(RUNX1-CBF2T1) fusion genes. The HL-60 cell line is Myc-positive. OCI-AML3 and HL-60 cell lines were cultured in basic medium of IMDM·15% FBS·1% P/S, Molm-13, NB4 and Kasumi-1 cell lines were cultured in basic medium of RPMI-1640 ·15% FBS·1% P/S. To induce the differentiation of undifferentiated leukemia cells, 10 ng/ml SCF, 10 ng/ml Flt3L, 10 ng/ml IL-3, 20 ng/ml GM-CSF, 50 ng/ml of G-CSF and 20 ng/ml EPO were added into the basic medium. Cell counts of all the cell lines were counted 1 week after the treatment of TDE (1 μM). The AML patients (AML-M3 subtypes without detecting the gene mutation) bone marrow derived CD34 + HSPCs and cord blood derived CD34 + HSPCs were isolated and cultured in described medium for 2 weeks with TDE treatment. Flow cytometry was performed to assess the differentiation of the OCI-AML3 cell line and AML derived CD34 + HSPCs using CD34, CD15 and CD66b.

Western blot assay of ELK1 or p-ELK1

Twenty million cells (either mouse total bone marrow cells or AML cell lines (with or without TDE treatment)) were used to extract total proteins using Radio Immunoprecipitation Assay (RIPA) Lysis Buffer (Beyotime, P0013B) with protease and phosphatase inhibitors (Beyotime, P1046). Cytoplasmic and nuclear proteins are extracted by the Nuclear and Cytoplasmic Protein Extraction Kit (Beyotime, P0028). The supernatant was collected by centrifugation (13,000 g; 15 min; 4 °C). Loading buffer (Catlog: ZS306-2) was added to the supernatant, and proteins were denatured by heating in a 95℃-water bath for 10 min. The denatured protein samples were separated by SDS-PAGE gel (Catlog: ZDTG-420T) at 180 V for 1 h. Proteins were transferred from the SDS-PAGE gel to a nitrocellulose (NC) membrane using the ACE S-Trans machine with parameters of 26 V and 600 S. Nonspecific binding sites were blocked with 5% non-fat milk powder or bovine serum albumin (BSA; for phosphorylation assays) in Tris-buffered saline with Tween-20 (TBST, Yeasen, Catlog:60145ES80) for 1.5 h. After blocking, the blots were incubated overnight at 4 ℃ with primary antibodies (Anti-ELK1 polyclonal Antibody (Biorbyt, Catlog: orb626705), anti-p-ELK1 polyclonal Antibody (phosphor-ELK1-S383 rabbit pAb, Catlog: AP0033) or anti-GAPDH polyclonal Antibody (Biosharp, Catlog: BL006B) diluted 1:1000 in blocking solution. The blots were then washed three times with TBST and incubated for 1.5 h with Goat Anti-Rabbit IgG (H + L) antibody (HRP) antibody (Biorbyt, Catlog: orb1176161) diluted 1:2000 in blocking solution. Proteins bands were detected using BeyoECL Plus (Beyotime, P0018S) on a Tanon Chemi Dog Ultra imaging system.

qPCR analysis

Total RNA from bone marrow samples or AML cell lines was extracted using GREENspin Fast Animal Tissue/Cell Total RNA Kit (Zomanbio, Catalog: ZP441-1). Subsequently, 1 μg of total RNA was used to synthesize cDNA with the HisyGo All-in-One RT Red SuperMix for qPCR (+ gDNA Wiper) Kit (Vazyme, Catalog: RT333-01). The qPCR assays were performed using ChamQ Universal SYBR qPCR Master Mix Kit (Vazyme, Catalog: Q711). Primers for detecting target gene expression are provided in Supplementary Table 1. Relative expression of the detected genes were calculated as 2^(-△Ct) or 2^(-△△Ct), where △Ct = Ct(target gene)-Ct(housekeeping gene B2M); △△Ct=△Ct(Treated sample)- △Ct(Ctrl sample).

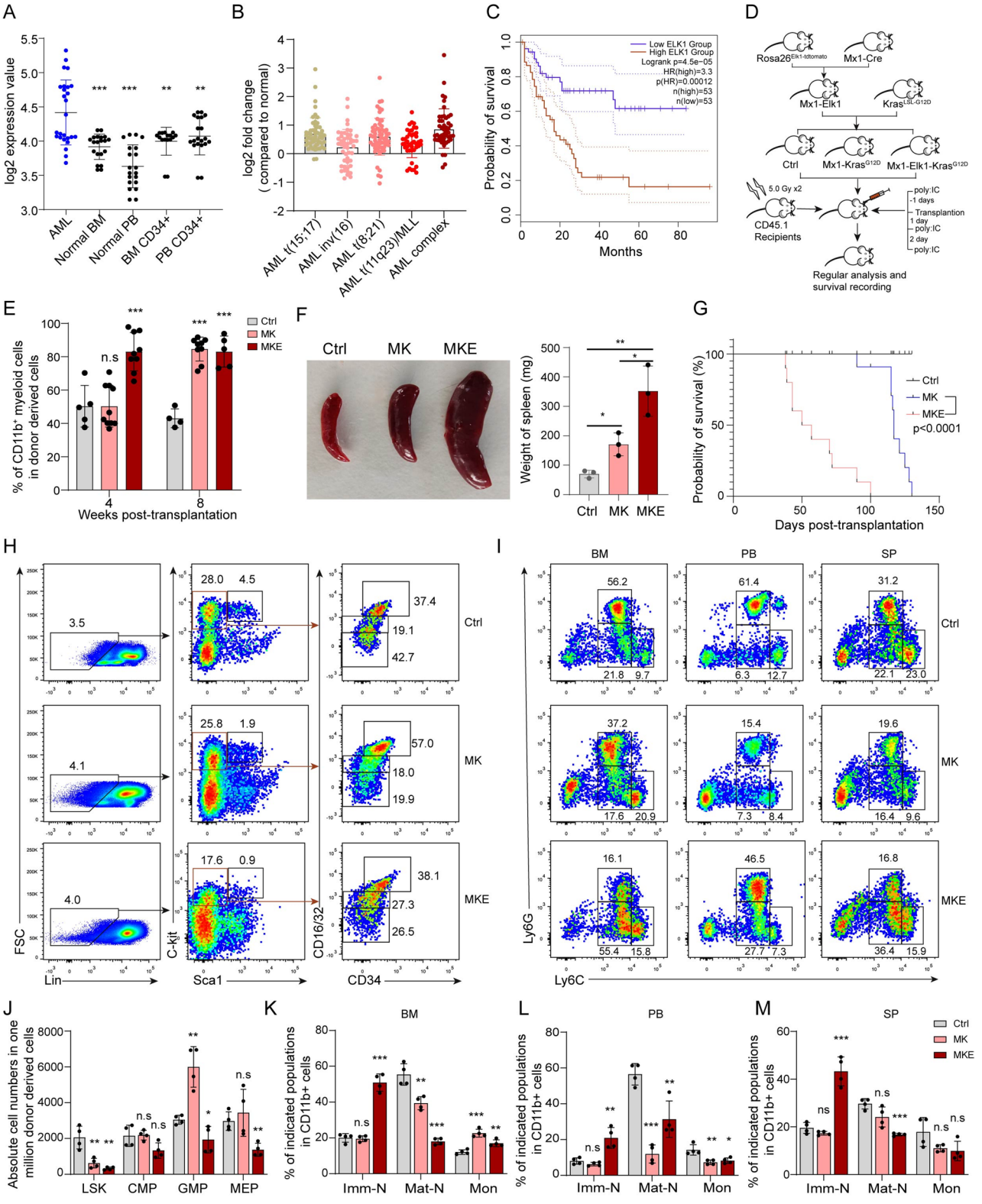

Fig. 1 (See legend on next page.)

(See figure on previous page.)

Fig. 1 Elk1 promotes KrasG12D-induced myeloid neoplasm progression. (A) Expression level of ELK1 in hematopoietic cells from healthy and AML donors (Data from GDS3057/210376_x_at). (B) Expression fold change of ELK1 in different types of AML compared to normal (data derived from BloodSpot (fobinf.com) 210850_s_at). (C) Overall survival of AML patients with high (top 50%) and low (bottom 50%) ELK1 expression. (D) Schematic diagram illustrating the impact of overexpressing Elk1 in KrasG12D-induced leukemogenesis. 1×10^6 total bone marrow cells from littermate control (Ctrl), Mx1-KrasG12D (MK) and Mx1-Elk1-KrasG12D (MKE) mice were used for transplantation. Polyinosinic–polycytidylic acid sodium salt (PolyIC) was injected with 3 doses into all the recipients via intraperitoneal injection every other day. (E) Statistical analysis of the percentages of $CD11b^+$ cells in the peripheral blood of recipients at 4 and 8 weeks after transplantation. Ctrl = 5 mice, MK = 10, MEK = 10, n.s, no significance. $^{***}P < 0.001$.(F) Statistical analysis of spleen weights of Ctrl, MK and MKE transplanted recipients. Recipient mice were sacrificed 8 weeks post-transplantation. (G) Kaplan–Meier survival curves of Ctrl, MK and MKE recipient mice. (H) Representative flow cytometry plots of myeloid progenitors in the bone marrow of Ctrl, MK and MKE transplanted recipients 8 weeks post-transplantation. (I) Representative flow cytometry plots of mature neutrophils, immature neutrophils and monocytes in the bone marrow, peripheral blood and spleen of Ctrl, MK and MKE transplanted mice. (J) Statistical analysis of the absolute cell numbers of hematopoietic progenitors in bone marrow of Ctrl, MK and MKE transplanted recipients. Ctrl = 4 mice, MK = 4 mice, MEK = 4 mice, n.s, no significance. $^{**}P < 0.01$, $^{***}P < 0.001$, $^{****}P < 0.0001$. (K-M) Statistical analysis of the percentages of $CD11b^+$ myeloid cell-derived immature neutrophils and mature neutrophils in bone marrow (K), peripheral blood (L) and spleen (M) of Ctrl, MK and MKE recipients. The data in panels (A, E, F, J-M) are presented as the mean ± SD. An unpaired Student's t-test (two-tailed) was performed. $N = 3$–9 mice; n.s, no significance. $^{**}P < 0.01$, $^{***}P < 0.001$, $^{****}P < 0.0001$

ShRNA knocking down of ELK1

Knocking down of ELK1 in AML cell lines was mediated by short hairpin RNA (shRNA). The target sequence of ELK1 (GCCTTGCGGTACTACTATGACA) was inserted into the lentiviral expression vector and the lentivirus was prepared using 293T cells as previous reported [22, 28].

Statistical analysis

The R packages of edgeR, DESeq2, clusterProfiler, pcaMethods, gplots, reshape2, ggplot2, Seurat, monocle2, GSEA, cluster, factoextra, uwot and sincell were used to perform statistical analysis of RNA-Seq data. Other significant analyses were performed using unpaired Student's t-tests (GraphPad Prism, GraphPad Software).

Data Availability

All the RNA-Seq data are deposited in NCBI's Gene Expression Omnibus (GEO) dataset with the accession number GSE299179. Other data supporting this study and materials are available from the corresponding author upon request.

Results

Overexpression of Elk1 accelerates the progression of KrasG12D mutation induced myeloid neoplasm

Generally, in the diagnosis of AML, multiple gene mutations tend to have a poorer prognosis and a higher recurrence rate than single gene mutations. This is mainly because different genes play different roles in hematopoietic development and cell proliferation, thus exerting distinct effects in the pathogenesis of AML. Eventually, these different effects will superimpose to promote or exacerbate leukemia onset. Here, we found that the expression of Elk1 is positively correlated with genes commonly mutated in AML [29, 30], such as KDM6A, KDM6B, KMT2A, KMT2B, DNMT3A, MLLT3, MLLT10, MLLT11, PML, IDH1, KRAS and NRAS (Supplementary Fig. 1A), and negatively correlated with neutrophil signature genes [22, 31], including CEBPE, MPO, ELANE and GF1I (Supplementary Fig. 1B). Given that undifferentiated lineage cells are common in leukemia, immature neutrophils accumulate in several types of AML. For example, the proportions of $CD15^+CD66b^-$ immature neutrophils exceed 95% in OCI-AML2 and OCI-AML3 AML cell lines (Supplementary Fig. 1C). Our previous study demonstrated that upregulation of ELK1 impedes the differentiation of neutrophils and leads to the accumulation of $CD15^+CD66b^l$ cells derived from human hematopoietic stem and progenitor cells (HSPCs) [22]. Thus, we suspect that ELK1 plays an important role in the progression of myeloid leukemia.

Interestingly, we found that ELK1 is highly expressed in AML cells compared to total bone marrow cells and HSPCs (Fig. 1A). Moreover, this upregulation is common for different types of AML with various cytogenetic abnormalities (Fig. 1B). Furthermore, patients with elevated ELK1 expression had a significantly shorter survival time than those with low expression (Fig. 1C). These results suggest that ELK1 may play a vital role in the development of AML. To confirm that the upregulation of ELK1 promotes the development of myeloid proliferative neoplasm, we constructed Elk1 conditional overexpression mice and mated with Mx1-Cre mice to confirm the expression level of Elk1 by qPCR and western blot (Supplementary Fig. 1 D-E) and then breed with the KrasG12D conditional overexpression mice to activate the ectopic expression of Elk1 and KrasG12D in the hematopoietic system. We transplanted total bone marrow cells from Mx1-Cre, $KrasG12D^{LSL/+}$, $Elk1^{LSL/+}$ mice (MKE) and analyzed the peripheral blood and survival of recipient mice (Fig. 1D). As expected, ectopic expression of ELK1 increased the proportion of $CD11b^+$ total myeloid cells, induced splenomegaly and increased the mortality of MKE recipient mice (Fig. 1E-G). Moreover, the ectopic expression of ELK1 reduced the percentages of LSK, GMP and MEP, leading to the depletion of mature neutrophils, as well as the accumulation of immature neutrophils in the bone marrow, spleen and peripheral blood (Fig. 1H-M, Supplementary Fig. 1F). In summary,

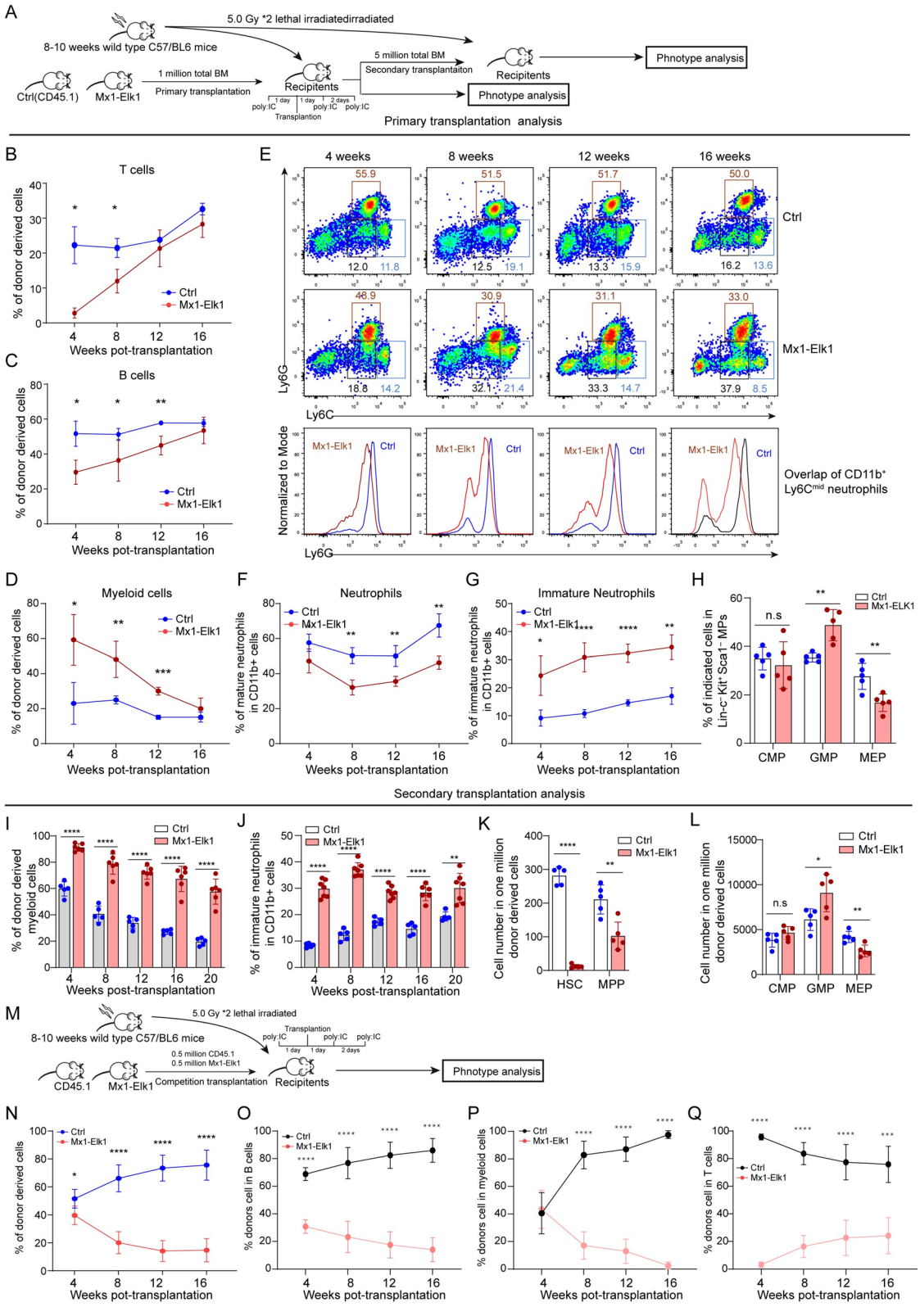

Fig. 2 (See legend on next page.)

(See figure on previous page.)

Fig. 2 Elk1 impedes neutrophil maturation and impairs HSC function under physiological conditions. (A) Schematic diagram showing the non-competition transplantation assay of Mx1-Elk1 and Ctrl mice. One million bone marrow cells of $Elk1^{LSL/+}$; Mx1-Cre mice were used for primary competitive transplantation. Five million bone marrow cells were transplanted to each recipient for secondary transplantation. (B-D) Statistical analysis of Mx1-Elk1 and Ctrl mice derived T cells (A), B cells (B) and myeloid cells (C) in peripheral blood of primary recipients at various time points after transplantation. Ctrl = 5 mice, Mx1-Elk1 = 5 mice, n.s, no significance. $^{**}P < 0.01$, $^{***}P < 0.001$, $^{****}P < 0.0001$. (E) Representative flow cytometry plots showing mature neutrophils ($Ly6C^{mid}Ly6G^{hi}$), immature neutrophils ($Ly6C^{mid}Ly6G^{low/-}$), and monocytes ($Ly6C^{hi}Ly6G^{low/-}$) and the expression level of Ly6G in $CD11b^+$ $Ly6C^{middle}$ cells in the peripheral blood of Mx1-Elk1 and Ctrl recipients. (F-G) Statistical analysis of neutrophils (E) and immature neutrophils (F) at various time points in peripheral blood of Mx1-Elk1 and Ctrl recipients. Ctrl = 5 mice, Mx1-Elk1 = 5 mice, n.s, no significance. $^{**}P < 0.01$, $^{***}P < 0.001$, $^{****}P < 0.0001$. (H) Statistical analysis of CMPs, GMPs and MEPs in bone marrow of Mx1-Elk1 and Ctrl recipients at 16 weeks post-transplantation. Ctrl = 4 mice, Mx1-Elk1 = 4 mice, n.s, no significance. $^{**}P < 0.01$. (I-J). Statistical analysis of $CD11b^+$ myeloid cells (H) and $CD11b^+$ myeloid cells -derived immature neutrophils in the peripheral blood of secondary transplanted recipients (I). Ctrl = 5 mice, Mx1-Elk1 = 7 mice, n.s, no significance. $^{**}P < 0.01$, $^{****}P < 0.0001$. (K-L) Statistical analysis of HSCs, MPPs (J) and CMPs, GMPs, MEPs (K) in the bone marrow of secondary transplanted recipients at 20 weeks post-transplantation. Ctrl = 5 mice, Mx1-Elk1 = 5 mice, n.s, no significance. $^{*}P < 0.05$, $^{**}P < 0.01$, $^{****}P < 0.0001$. (M) Schematic diagram showing the competition transplantation analysis procedure. 0.5 million total bone marrow of CD45.1 or Mx1-Elk1 mice were transplanted into 5.0 Gy*2 lethal irradiation treated recipients (CD45.2), flow cytometry analysis was performed at 4, 8, 12, 16 weeks post transplantation. (N-Q) Statistical analysis of the percentages of donor derived total nucleated cells (L), $CD19^+$ B cells (M), $CD11b^+$ myeloid cells (N) and $CD3^+$ T cells (O) *in recipients*. Ctrl = 7 mice, Mx1-Elk1 = 7 mice, n.s, no significance. $^{*}P < 0.05$, $^{**}P < 0.01$, $^{***}P < 0.001$, $^{****}P < 0.0001$. The data in panels (B-D, F-L, N-Q) are presented as the mean ± SD. An unpaired Student's t-test (two-tailed) was performed

the upregulation of ELK1 accelerates KrasG12D-induced myeloid proliferative neoplasm, while impeding neutrophil maturation.

Conditional ectopic expression of Elk1 impairs the stemness of HSCs and blocks neutrophil differentiation and maturation in vivo

Knockout of Elk1 was reported to show normal T cell immune response in mouse model [32]. On the other hand, our previous studies demonstrated that upregulation of ELK1 blocks erythrocyte lineage differentiation at the CMP stage and neutrophil maturation at the late stage with a hematopoietic stem/progenitors cell based in vitro differentiation model [20, 22]. Nevertheless, the role of ELK1 in hematopoiesis remains to be fully explored. To explore the roles of ELK1 in hematopoiesis in vivo, we aimed to examine the effects of Elk1 in primary and secondary recipient mice (Fig. 2A). First, bone marrow from Mx1-Elk1 mice were transplanted into lethally irradiated recipients and peripheral blood (PB) of recipient mice was then regularly monitored for lineage differentiation. The results indicated that the proportions of B cells and T cells were significantly lower than those of the control group at 4–8 weeks post-transplantation and became comparable to control at 16 weeks post-transplantation (Fig. 2B-C). In contrast, a significantly higher proportion of $CD11b^+$ myeloid cells were observed from 4 to 12 weeks post-transplantation and became comparable to control (Fig. 2D). Subsequently, we analyzed the proportions of mature ($CD11b^+Ly6C^{mid}Ly6G^{hi}$) and immature neutrophils ($CD11b^+Ly6C^{mid}Ly6G^-$). At all time points, we observed a significantly lower proportion of mature neutrophils and a significantly higher proportion of immature neutrophils in the PB of recipients (Fig. 2E-G). Further analysis of myeloid progenitors in the bone marrow of Mx1-Elk1 transplanted recipients at 16 weeks post-transplantation revealed a significantly higher proportion of granulocyte-monocyte progenitors (GMP) and a lower proportion of megakaryocyte-erythrocyte progenitors (MEP) in Lin-$ckit^+Sca1^-$ myeloid progenitor compartment (Fig. 2H, Supplementary Fig. 2A). A higher proportion of immature neutrophils was also observed in the spleen (SP) and bone marrow (BM) (Supplementary Fig. 2B-D) and donor derived-erythrocytes were merely detected (Supplementary Fig. 2E). We conducted secondary transplantation with 5 million total bone marrow cells of primary Mx1-Elk1 recipients to determine whether overexpression of Elk1 would affect self-renewal and lineage specification in a more stressed condition. Significantly increased percentages of $CD11b^+$ myeloid cells and $CD11b^+Ly6G^{low/-}Ly6C^{mid}$ immature neutrophils in $CD11b^+$ myeloid compartment were observed at all analysis points in secondary recipients (Fig. 2I-J). Lower proportions of donor-derived B cells, but not T cells, were detected in the PB (Supplementary Fig. 2F-G). Furthermore, we found that significantly lower proportions of hematopoietic stem cells (HSC) and multipotent progenitors (MPP) in the BM of Mx1-Elk1 secondary recipients (Fig. 2K). A significantly higher proportion of GMP and a lower proportion of MEP were observed in Lin-$ckit^+Sca1^-$myeloid progenitor cells of the secondary transplanted recipients (Fig. 2L). However, none of these recipient mice developed leukemia, which indicated that elevated Elk1 expression is insufficient to drive leukemia development.

Given the significantly lower proportions of HSC, MPP and decreased donor-derived cellularity in the secondary transplanted recipients (Fig. 2J, Supplementary Fig. 2H), we hypothesized that overexpression of Elk1 impairs the stemness and self-renewal of HSC. To validate this hypothesis, we performed a 1:1 competition transplantation of $CD45.2^+$ Mx1-Elk1 bone marrow cells with CD45.1 competitor cells (Fig. 2M). The results demonstrated that the proportions of Mx1-Elk1-derived total leukocytes, $CD11b^+$ myeloid cells, $CD3^+$ T cells and $CD19^+$ B cells were all significantly lower in the PB of

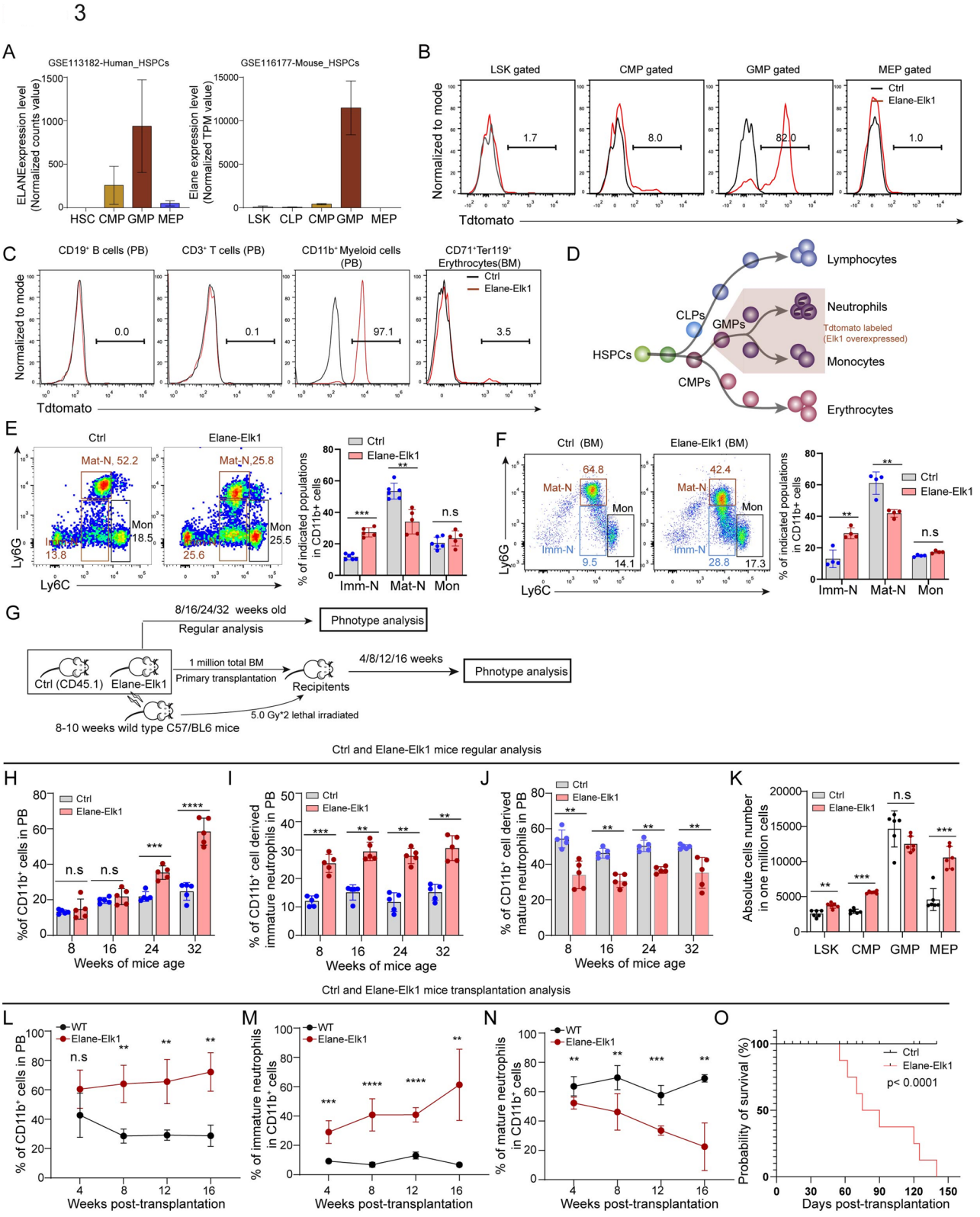

Fig. 3 (See legend on next page.)

(See figure on previous page.)

Fig. 3 Ectopic expression of Elk1 at myeloid progenitor level leads to the depletion of mature neutrophils under transplantation stress. (A) Statistical analysis of ELANE expression level in different human and mouse hematopoietic progenitors. Five replicates for each human hematopoietic stem/progenitor cell populations (GSE113182), two replicates for each mouse hematopoietic stem/progenitor cells populations (GSE116177). (B) Representative flow cytometry plots showing the percentages of Elk1 overexpressing cells (Tdtomato+) in LSKs, CMPs, GMPs and MEPs in bone marrow of Elane-Elk1 mice. (C) Representative flow cytometry plots showing the percentages of Elk1 overexpressing cells (Tdtomato$^+$) in peripheral blood CD19$^+$ B cells, CD3$^+$ T cells, CD11b$^+$ myeloid cells and bone marrow derived CD71$^+$Ter119$^+$ erythroid cells of Elane-Elk1 and littermate control mice. (D) Schematic diagram showing that Elk1 is specifically expressing in myeloid progenitors and myeloid lineages in Elane-Elk1 mice. (E-F) Flow cytometry analysis of CD11b$^+$ derived Ly6G$^{low/-}$Ly6C^{mid} immature neutrophils, Ly6G^{high}Ly6C^{mid} mature neutrophils and monocytes in peripheral blood (E) and bone marrow (F) of Elane-Elk1 mice or littermate control mice. Ctrl = 4–6 mice, Elane-Elk1 = 4–5 mice. n.s, no significance. $^{**}P < 0.01$, $^{***}P < 0.001$. (G) Schematic diagram showing the regular analysis of Elane-Elk1 transgenic mice at the age of 8, 16,24, 32 weeks and non-competition transplantation assay of Elane-Elk1 and Ctrl mice. One million bone marrow cells of Elane-Elk1 mice were used for primary non-competitive transplantation, and cytometry analysis was performed at 4, 8, 12, 16 weeks post-transplantation. (H-J) Statistical analysis of CD11b$^+$ myeloid cells (G), Ly6G$^{int/-}$Ly6C^{mid} immature neutrophils (H) and Ly6G$^{high/-}$Ly6C^{mid} mature neutrophils in peripheral blood of Elane-Elk1 mice or littermate control (Ctrl) mice at different weeks. Ctrl = 5 mice, Elane-Elk1 = 5 mice, n.s, no significance. $^{**}P < 0.01$, $^{***}P < 0.001$. (K) Statistical analysis of LSKs, GMPs, CMPs and MEPs in the bone marrow of Elane-Elk1 mice or littermate control (Ctrl) mice at 40 weeks of age. Ctrl = 6 mice, Elane-Elk1 = 5 mice, n.s, no significance. $^{**}P < 0.01$, $^{***}P < 0.001$. (L-N) Statistical analysis of CD11b$^+$ gated mature neutrophils (K), immature neutrophils (L) and total myeloid cells (M) in peripheral blood of Elane-Elk1 and littermate control recipient mice. Ctrl = 5 mice, Elane-Elk1 = 7 mice, n.s, no significance. $^{**}P < 0.01$, $^{***}P < 0.001$. (O) Survival curve of Elk1-Elane and littermate control recipients. Ctrl = 5 mice, Elane-Elk1 = 8 mice. The bar plots (E-F, H-N) are presented as the mean ± SD. An unpaired Student's t-test (two-tailed) was performed

all recipients (Fig. 2N-Q). Moreover, Mx1-Elk1-derived LSK, CMP, GMP, MEP and Lin$^+$ cells in bone marrow also failed to compete with competitor cells and comprised less than 20% of respective compartment (Supplementary Fig. 2I-J). Collectively, these data indicate that upregulation of Elk1 impairs the stemness of HSC, disrupts erythropoiesis, and hinders the maturation of neutrophils.

Ectopic expression of Elk1 in GMP blocks neutrophil maturation and leads to neutropenia

To investigate the role of Elk1 in the maturation of neutrophils without compromising the stemness of HSCs, we employed Lyz2-Cre to induce the ectopic expression of Elk1 specifically in CD11b$^+$ myeloid cells. Intriguingly, our results showed that Lyz2-Cre driven Elk1 expression did not affect myeloid cell differentiation or neutrophil maturation (Supplementary Fig. 3A-G). Subsequently, we found that *Elane* is specially highly expressed in both human and mouse GMPs, but not in CMPs or MEPs (Fig. 3A). Thus, we crossed Elane-Cre mice with Elk1$^{LSL/+}$ mice to generate Elane-Elk1 mice. Flow cytometry analysis showed that more than 80% of GMPs were tdtomato$^+$, about 8% of CMPs were tdtomato$^+$. In contrast, only 1% of MEPs were tdtomato$^+$ (Fig. 3B). Additionally, over 97% of CD11b$^+$ myeloid cells were tdtomato$^+$, while only 3.5% of CD71$^+$Ter119$^+$ nucleated erythrocytes were tdtomato$^+$ (Fig. 3C). These results confirmed that Elane-Cre could efficiently drive Elk1 overexpression in GMPs (Fig. 3D).

To assess whether Elk1 upregulation in GMPs hinders the maturation of neutrophils, we first examined the immature neutrophils and mature neutrophils in the peripheral blood and bone marrow of Elane-Elk1 mice. The results showed a significant increase of immature neutrophils and decrease of mature neutrophils both in the peripheral blood and bone marrow (Fig. 3E-F). These data confirmed that Elk1 overexpression in GMPs effectively blocked neutrophil maturation.

To further investigate the impact of blocking neutrophil maturation, we dynamically analyzed the CD11b$^+$ myeloid cells and immature neutrophils in peripheral blood (PB) of the Elane-Elk1 mice from 8 to 32 weeks of age and performed transplantation analysis (Fig. 3G). A significantly higher proportion of total CD11b$^+$ myeloid cells were observed from 24 to 32 weeks and significantly increased immature neutrophils and decreased mature neutrophils were detected at all time points in PB (Fig. 3H-J). Interestingly, only increased LSK, CMP, MEPs were detected in the bone marrow of Elane-Elk1 mice, but not GMPs (Fig. 3K, Supplementary Fig. 4A).

Despite the elevation of total CD11b$^+$ myeloid cells detected in the Elane-Elk1 mice (Fig. 3H), these mice did not develop myeloid neoplasm. To further analyze whether bone marrow transplantation-induced stressed hematopoiesis would accelerate the exhaustion of myeloid progenitor cells and affect survival, we transplanted the bone marrow of Elane-Elk1 mice into lethally irradiated recipient mice and analyzed the proportions of myeloid cells, mature neutrophils, and immature neutrophils in the peripheral blood of the recipient mice every four weeks after transplantation. The results showed that the proportion of CD11b$^+$ total myeloid cells and immature neutrophils in the PB of Elane-Elk1 transplant recipient mice was significantly higher than control, and the proportion of mature neutrophils decreased with time (Fig. 3L-N, Supplementary Fig. 4B-C). Meanwhile, we detected a significant decrease in GMPs, indicating exhaustion of GMPs to compensate for the lack of mature neutrophils (Supplementary Fig. 4D-E). At the same time, we found that Elane-Elk1 recipient mice began to die at 8 weeks post-transplantation, and all these recipients had a significantly shorter lifespan (Fig. 3O). The death of these mice was mainly manifested by the lack of

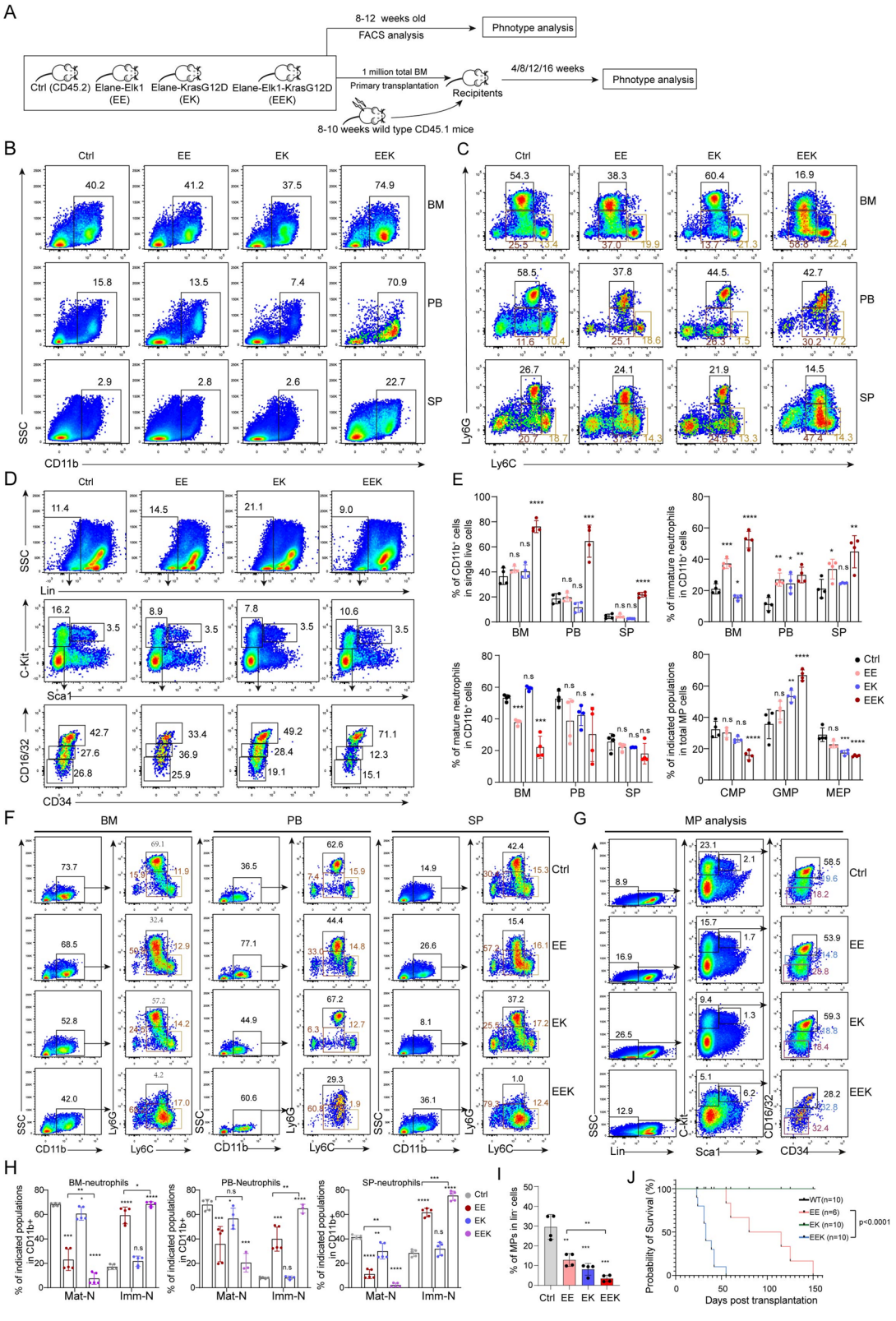

Fig. 4 (See legend on next page.)

(See figure on previous page.)

Fig. 4 Impeding neutrophil maturation promotes KrasG12D-induced myeloid proliferative neoplasm development. (A) Schematic diagram showing the phenotype analysis of Elane-Elk1-KrasG12D, Elane- KrasG12D and Elane-Elk1 transgenic mice at the age of 8–10 weeks and non-competition transplantation assay of Elane-Elk1-KrasG12D, Elane- KrasG12D and Elane-Elk1. One million bone marrow cells of Elane-Elk1-KrasG12D, Elane- KrasG12D, Elane-Elk1 and littermate control mice were used for primary non-competitive transplantation, and flow cytometry analysis was performed at 4–6 weeks post-transplantation (prior to mouse death). (B-D) Representative flow cytometry plots showing $CD11b^+$ myeloid cells (A), $CD11b^+$ gated $Ly6G^+Ly6C^{mid}$ mature neutrophils and $Ly6G^{int/-}Ly6C^{mid}$ immature neutrophils in bone marrow (BM), peripheral blood (PB) and spleen (SP) (B), and GMPs, CMPs, MEPs in total myeloid progenitors in bone marrow (C) of 8-weeks-old Elane-Elk1(EE), Elane-KrasG12D (EK), Elane-Elk1-KrasG12D (EEK) and littermate mice. (E) Statistical analysis of the percentages of $CD11b^+$ myeloid cells, $CD11b^+$ gated $Ly6G^+Ly6C^{mid}$ mature neutrophils and $Ly6G^{int/-}Ly6C^{mid}$ immature neutrophils in bone marrow (BM), peripheral blood (PB) and spleen (SP), and GMPs, CMPs, MEPs in total myeloid progenitors in bone marrow of EE, EK, EEK and littermate mice. Ctrl = 4 mice, Elane-Elk1(EE) = 4 mice, Elane-KrasG12D (EK) = mice, Elane-Elk1-KrasG12D (EEK) = 4mice. n.s, no significance. $^*P < 0.05$,$^{**}P < 0.01$, $^{***}P < 0.001$, $^{****}P < 0.0001$. (F-G) Representative flow cytometry plots showing $CD11b^+$ gated $Ly6G^+Ly6C^{mid}$ mature neutrophils and $Ly6G^{int/-}Ly6C^{mid}$ immature neutrophils in bone marrow (BM), peripheral blood (PB) and spleen (SP), and LSKs, GMPs, CMPs and MEPs in bone marrow of EE, EK, EEK and littermate mice transplanted recipients

(H) Statistical analysis of the percentages of $Ly6G^+Ly6C^{mid}$ mature neutrophils and $Ly6G^{int/-}Ly6C^{mid}$ immature neutrophils in $CD11b^+$ myeloid cells derived from bone marrow (BM), peripheral blood (PB) and spleen (SP) of EE, EK, EEK and littermate mice transplanted recipients. Ctrl = 5 mice, Elane-Elk1(EE) = 5 mice, Elane-KrasG12D (EK) = 4 mice, Elane-Elk1-KrasG12D (EEK) = 5 mice. n.s, no significance. $^*P < 0.05$,$^{**}P < 0.01$, $^{***}P < 0.001$, $^{****}P < 0.0001$. (I) Statistical analysis of the percentages of Lin^- C-kit^+Sca1- myeloid progenitors in Lin- cells derived from the bone marrow of EE, EK, EEK and littermate mice transplanted recipients. Ctrl = 4 mice, Elane-Elk1(EE) = 4 mice, Elane-KrasG12D (EK) = 4 mice, Elane-Elk1-KrasG12D (EEK) = 4 mice. $^{**}P < 0.01$, $^{***}P < 0.001$. (J) Kaplan–Meier survival curves of EE, EK, EEK and littermate mice transplanted recipients. Ctrl = 6 mice, Elane-Elk1(EE) = 6 mice, Elane-KrasG12D (EK) = 10 mice, Elane-Elk1-KrasG12D (EEK) = 10 mice. The bar plots (E, H, I) are presented as the mean ± SD. An unpaired Student's t-test (two-tailed) was performed

mature neutrophils. No extramedullary hematopoiesis or splenomegaly was observed in the recipients. These findings suggested that repopulation stress exacerbates the Elk1-induced exhaustion of myeloid progenitors and neutropenia.

Hindering neutrophils maturation promotes myeloid proliferative neoplasm development

To dissect the roles of Elk1 in myeloid neoplasm development, we crossed Elane-Elk1 mice with KrasG12D mice to generate Elane-Elk1-KrasG12D triple-transgenic mice. Flow cytometry assays were performed to analyze neutrophils and immature neutrophils in peripheral blood, spleen and bone marrow, as well as myeloid progenitors in the bone marrow of these transgenic mice or transplanted recipients (Fig. 4A). The results revealed that significantly higher proportions of $CD11b^+$ total myeloid cells, $CD11b^+Ly6G^{-/low}Ly6C^{mid}$ immature neutrophils and GMPs were detected in Elane-Elk1-KrasG12D mice compared to Elane-Elk1 or Elane-KrasG12D mice. Conversely, CMPs, MEPs and mature neutrophils were significantly reduced in the bone marrow of Elane-KrasG12D mice (Fig. 4B-E).

To further investigate the impact of Elk1 on KrasG12D mutation-induced myeloid proliferative neoplasm, we performed non-competitive bone marrow transplantation using Elane-Elk1-KrasG12D, Elane-Elk1, Elane-KrasG12D and littermate control mice. Surprisingly, the KrasG12D mutation in GMPs only modestly changes the proportions of mature neutrophils in BM, PB and SP 4 weeks post-transplantation and not affect the survival of all the recipients (Elane-KrasG12D group compared to Ctrl group) (Fig. 4F-H). Interestingly, the cooperation between KrasG12D mutation and Elk1 overexpression accelerated the depletion of mature neutrophils (Fig. 4F-H, Elane-Elk1 group compared to Elane-Elk1-KrasG12D group). Notably, rare mature neutrophils were detected in peripheral blood, spleen and bone marrow of the Elane-Elk1-KrasG12D transplantation recipients, while the proportion of immature neutrophil increased significantly (Fig. 4F-H). Additionally, the exhaust of myeloid progenitors (MP) in Elane-Elk1-KrasG12D transplanted recipients was more serious than Elane-Elk1 or Elane-KrasG12D transplanted recipients (Fig. 4I). Finally, all Elane-Elk1-KrasG12D recipients died within 55 days, while Elane-Elk1 transplanted recipients survived between 56 to150 days due to the absence of mature neutrophils (Figs. 3O and 4J). These findings indicate that Elk1 overexpression obstructs neutrophil maturation, exacerbating neutropenia in myeloid proliferative neoplasm model.

The Elk1 regulated signal pathways in hematopoietic hierarchy

To dissect the signal pathways altered by the upregulation of Elk1 in different hematopoiesis stages, we sorted $CD3/CD19/NK1.1/Ter119^-CD11b^+C\text{-}kit^-$ and $CD3/CD19/NK1.1/Ter119^-CD11b^-C\text{-}kit^+$ cells containing HSC, MPP, CMP, GMP, MEPs, monocyte progenitors (MoPs), neutrophil progenitor (NP), immature neutrophil and mature neutrophil from the bone marrow of Mx1-Elk1 and wild type control mice (Fig. 5A) for single cell RNA sequencing. Representative markers Mecom, Pf4, Cd34, Kit, Flt3, Il7r, Epor, Cd55, Gypa, Mpo, Cebpe, Elane, Itgam, Ly6g and Csf1r were used to identify the HSCs, MPPs, CLPs, CMPs, GMPs, MEPs, MoPs, NPs and neutrophils from the single cell data (Supplementary Fig. 5A-B, Fig. 5B). Gene ontology enrichment analysis was performed for the differential expressed genes (DEGs) in HSCs, MPPs, GMPs, NPs, N1(immature neutrophils) and N2 (mature neutrophils). The results showed that the DEGs were mainly related to

homeostasis, myeloid lineage differentiation, cell chemotaxis and myeloid cell activation pathways (Supplementary Fig. 5C). Notably, Hlf, Basp1 and Hoxa9 related to the stemness of HSCs [33–35] and Ly6g related to neutrophil differentiation were downregulated in Mx1-Elk1 group (Fig. 5C).

To further validate the pathways changed by Elk1, we sorted LSK, CMP, GMP and mature neutrophils for transcriptomic analysis. Unsupervised cluster analysis of the bulk cell RNA sequencing data of LSKs, CMPs, GMPs and mature neutrophils showed that LSKs, CMPs, GMPs and mature neutrophils from Mx1-Elk1 mice still clustered with respective cellular compartments, indicating the upregulation of Elk1 did not completely change the transcriptome of each cell populations (Supplementary Fig. 5D). To identify the essential pathways upregulated by Elk1 at different stages, GSEA (Gene Set Enrichment Analysis) was performed. The results showed that Elk1 upregulated the granulocyte chemotaxis and granulocytopoietic cell aging signals in LSKs, downregulated the granulocytopoietic cell aging and precursor cell aging pathways in CMPs, upregulated the TNF-α and inflammatory response signals in GMPs, and upregulated E2F targets and translation pathways in mature neutrophils (Fig. 5D). The GO enrichment analysis of the DEGs indicated that the upregulation of Elk1 upregulated the leukocyte migration, leukocyte proliferation and chemotaxis signals in LSKs, mononuclear cell proliferation-related pathway in CMPs and translation related signals in GMPs and mature neutrophils (Supplementary Fig. 5E). Heatmaps showed that Elk1 downregulated HSC homeostasis related-genes, such as Hoxa9, Hoxa10, Hlf, Gata2, and Mllt3 and upregulated the granulocyte differentiation-related genes, including Cebpe, Gfi1, Elane, Mpo and Prtn3 in LSKs (Fig. 5E(I)). However, Elk1 downregulated the granulopoiesis-related genes including Cebpe, Gfi1, Elane, Mpo and Prtn3 in CMPs (Fig. 5E(II)). Additionally, Elk1 upregulated myeloid differentiation genes, such as Egr1 and Egr3 in GMPs (Fig. 5E(III)). However, Elk1 upregulation during the terminal neutrophil maturation primarily upregulated the translation-related genes (Fig. 5E(IV)). Through integrated analysis of bulk-cell RNA sequencing and single-cell RNA sequencing data, we found that the expression of Hlf, a key regulatory gene for maintaining hematopoietic stem cell (HSCs) stemness [24], was drastically decreased in Mx1-Elk1 HSCs (Fig. 5F). Meanwhile, the expression of Egr1, a critical regulatory gene of HSC proliferation, localization [36], myeloid lineage differentiation and leukemia [37], was significantly upregulated in hematopoietic stem cells and myeloid progenitor cells (HSPCs) (Fig. 5G). Elk1 has been reported to be dispensable for the expression of Egr1 [38]. Collectively, these results indicate that Elk1 impairs HSCs stemness and normal hematopoiesis probably through downregulating Hlf and upregulating Egr1.

Dissecting the signals of neutrophil maturation by proteinomics

In the present study, less than 100 DEGs (padj (adjusted P-value) < 0.05) were identified in immature neutrophils using bulk-cell RNA sequencing. To further elucidate the mechanism by which Elk1 impedes neutrophil maturation, we sorted $CD11b^{+}Ly6C^{mid}Ly6G^{+}$ mature neutrophils and $CD11b^{+}Ly6C^{mid}Ly6G^{int/-}$ immature neutrophils (Fig. 6A) for proteomics analysis. The proteomics analysis revealed a total of over 2,000 differentially expressed proteins between mature and immature neutrophils (Fig. 6B). Gene Ontology (GO) enrichment analysis revealed that cell migration and chemokine signals were upregulated, while oxidative phosphorylation, cell cycle and DNA replication signals were downregulated during normal neutrophil maturation (Fig. 6C, Supplementary figure 6A). Notably, the ectopic expression of Elk1 upregulated several metabolic signaling pathways and pathways associated with neutrophil-extracellular trap (NET) formation, neutrophil migration and MAPK signaling pathways in immature neutrophils (Fig. 6C-D, Supplementary figure 6B). Interestingly, it downregulated oxidative phosphorylation, MAPK, MTOR, and ErbB signaling pathways in mature neutrophils (Fig. 6C).

From the list of differentially expressed proteins in immature and mature neutrophils, we identified 32 proteins that were upregulated by Elk1 in both immature and mature neutrophils (Fig. 6E-G). Only 5 out of 32 upregulated proteins were associated with the ERK signaling pathway (Fig. 6F). Intriguingly, this set of upregulated proteins included Lsp1, Trip4, Thbs1, and Ifitm3, which were genes associated with shorter survival in AML (Fig. 6H). Notably, three of these factors, Lsp1 [39], Thbs1 [40] and Ifitm3 [41] were reported to be novel prognostic and therapeutic targets for AML. These data indicate that Elk1 primarily hinders the differentiation and maturation of neutrophils by altering ERK pathways at the protein level, which leads to the accumulation of immature neutrophils and their functional abnormalities, ultimately results in the depletion of mature neutrophils.

Targeting ELK1 inhibits the proliferation of leukemia cells and promotes differentiation of leukemic stem cells to generate mature neutrophil

A previous report has shown that targeting the MEK signaling pathway significantly prolongs survival in patients with RAS-mutated AML [42]. ELK1, a downstream effector of ERK, has been identified as a potential therapeutic target for depression [43] with its peptide inhibitor TDE shown to mediate this therapeutic effect [44] by inhibit the translocation of ELK1 [44]. Thus, we

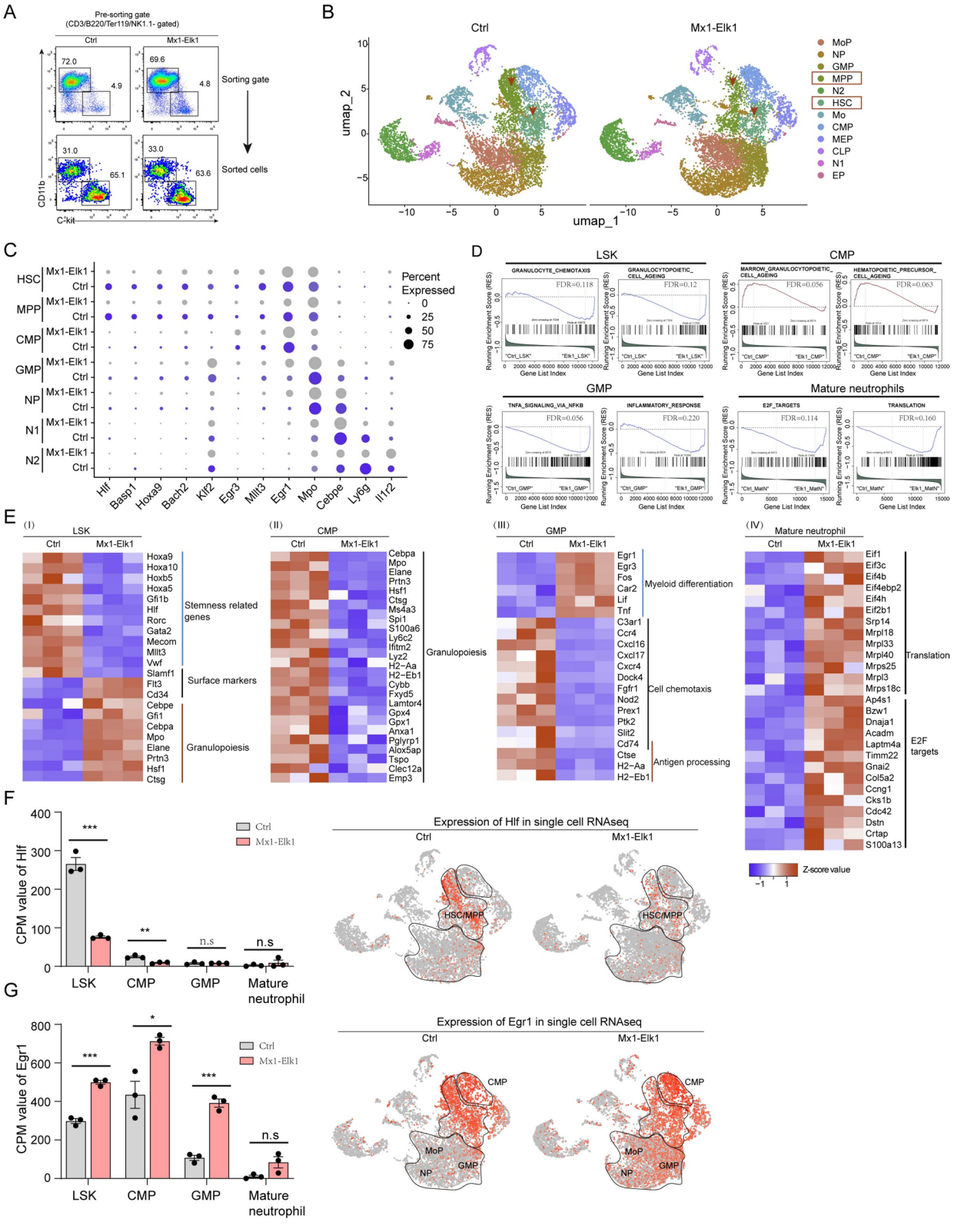

Fig. 5 (See legend on next page.)

(See figure on previous page.)

Fig. 5 Dissecting the molecular mechanism of Elk1 in regulating hematopoiesis. (A) Flow cytometry plots showing the sorting gate of CD3/CD19/NK1.1/Ter119$^-$CD11b$^+$C-kit$^-$ and CD3/CD19/NK1.1/Ter119$^-$CD11b$^-$C-kit$^+$ cells derived from Mx1-Elk1 and littermate control, and the ratio of these two cell populations in the samples for single-cell RNAseq. (B) UMAP showing the clusters of HSCs, MPPs, CMPs, GMPs, MEPs, CLPs, MoPs, NPs and neutrophils derived from the single-cell RNAseq data of CD3/CD19/NK1.1/Ter119$^-$CD11b$^+$C-kit$^-$ and CD3/CD19/NK1.1/Ter119$^-$CD11b$^-$C-kit$^+$ cells sorted from BM of Ctrl and Mx1-Elk1 mice. (C) Dotplot showing the representative differentially expressed genes in different cell clusters. (D) GSEA analysis showing the active signals in LSKs, CMPs, GMPs and mature neutrophils (FDR < 0.25). (E) Heatmaps showing the differentially expressed genes in LSKs, GMPs, CMPs and mature neutrophils. (F) Bar plots and UMAP plots showing the expression level of Hlf in different cell types derived from bulk RNA-seq and single-cell RNA-seq data. (G) Bar plots and UMAP plots showing the expression level of Egr1 in different cell types derived from bulk RNA-seq and single-cell RNA-seq data. HSCs, hematopoietic stem cells. MPPs, multipotent progenitors. CMPs, common myeloid progenitors. GMPs, granulocyte-monocyte progenitors. MEPs, megakaryocyte-erythroid progenitors. CLPs, common lymphoid progenitors. MoPs, monocyte progenitors. NPs, neutrophil progenitors

hypothesize that the ELK1 inhibitor TDE may be used to induce further differentiation of undifferentiated leukemia cells. First, we confirmed the expression levels of ELK1 in different AML cell lines via qPCR (Supplementary Fig. 7A) and western blot (Fig. 7A, Supplementary Fig. 7B). We also confirmed that TDE does not affect the phosphorylation of ELK1 (Supplementary Fig. 7C) but rather impairs the nuclear translocation of L-ELK1 (Supplementary Fig. 7D). We then investigated whether inhibiting ELK1 with its peptide inhibitor TDE could suppress leukemia cell proliferation and promote the maturation of immature neutrophils. The results showed that TDE effectively inhibited the proliferation of OCI-AML3, HL-60, Molm-13 cell lines (Fig. 7B) without affecting cell apoptosis, consistent with the results of ELK1 knockdown (Supplementary Fig. 7E-I). Most importantly, TDE induced the differentiation of CD15$^+$CD66b$^-$ OCI-AML3 leukemia cells into CD15$^+$CD66b$^+$ mature neutrophils (Fig. 7C). Subsequently, CD34$^+$ primary AML cells were isolated and sorted from bone marrow aspirates and cultured for 14 days with TDE to further evaluate the effects of ELK1 inhibition (Fig. 7D). Intriguingly, inhibiting ELK1 with TDE increased the proportion of CD15$^+$CD66b$^+$ mature neutrophils and suppressed the proliferation of CD34$^+$ leukemia stem cells (Fig. 7E-G).

To further confirm the downstream target genes of ELK1, we used qPCR to detect the hypothesized target genes (HLF, EGR1, LSP1, TRIP4, THBS1 and IFITM3) in human AML cell lines and ELK1- or KrasG12D- transgenic mice. The results showed that 5 out of 6 genes downregulated in OCI-AML3 cells treated with TDE, whereas only but only one or two of these six genes exhibited significantly changed in HL-60, Molm-13 and Kasumi-1 cell lines (Fig. 7H-L) or the bone marrow of ELK1- or KrasG12D- transgenic mice (Supplementary Fig. 7J). Additionally, treatment with TDE did not improve the persistence of early leukemia progenitor cells (Supplementary Fig. 7K). Overall, our study reveals a novel role of ELK1 in promoting myeloid leukemia by impairing neutrophil maturation; however, further studies on the mechanisms underlying the distinct roles of L-ELK1 and S-ELK1 in hematopoiesis and leukemogenesis are needed (Fig. 7M).

Discussion

Cell differentiation and proliferation are the main focus of the AML treatment. Overcome the disorder of lineage differentiation and maturation of leukemia cells would improve the function leukocytes. Currently, clinical guidelines for AML treatment indicate that its treatment mainly relies on chemotherapeutic drugs, which induce cell death, as well as bone marrow transplantation [1]. The approach of promoting the differentiation and maturation of undifferentiated cells has only been successfully applied in the treatment of APL (acute promyelocytic leukemia) using all-trans retinoic acid, achieving a 5-year overall survival rate of over 97% [45]. This suggests that treating AML by promoting the differentiation and maturation of undifferentiated cells is feasible. However, due to the lack of promising targets that specifically regulate the differentiation and maturation of monocytes or neutrophils, no new drugs have been developed to exert this strategy as to treat AML.

In this study, we discovered that ELK1 is highly expressed in different types of AML. Using the KrasG12D conditional overexpression mouse model, we found that Elk1 upregulation indeed promotes KrasG12D-induced myeloid leukemia through impeding neutrophil maturation but not impairing the self-renewal of HSCs. Upregulation of Elk1 expression impairs hematopoiesis at multiple hierarchical stages, including reducing the hematopoietic capacity of HSCs, promoting the differentiation of myeloid progenitor cells into granulocytes and monocytes, inhibiting the production of erythrocytes, and most importantly, inhibiting the differentiation and maturation of the neutrophil lineage. Under conditions of stressed hematopoiesis, ELK1 causes neutrophil deficiency by inhibiting neutrophil differentiation and induces death in mice, but the death of the mice is not due to the occurrence of myeloid neoplasm.

While ELK1 is one of the downstream genes of RAS-MAPK signal pathway, through single-cell and bulk-cell transcriptome sequencing analysis, the upregulation of Elk1 does not significantly change the MEK/ERK signaling pathway downstream of KrasG12D [46]. This suggests that Elk1 impairs the differentiation and maturation of neutrophils through mechanism independent of MEK/ERK signaling pathway. In addition, we also found

Figure 6

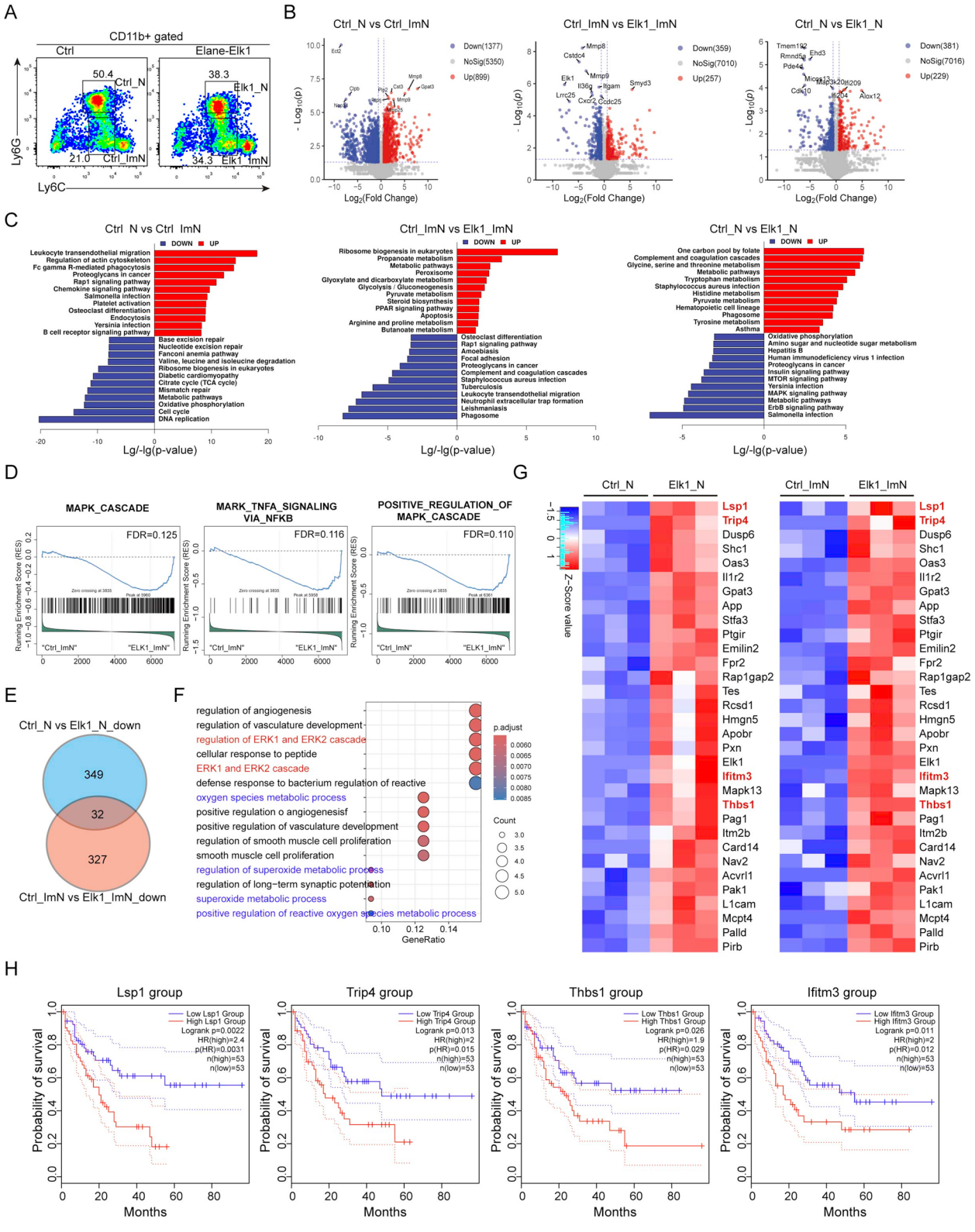

Fig. 6 (See legend on next page.)

(See figure on previous page.)

Fig. 6 Dissecting the signals upregulated in neutrophils by Elk1 via proteomics. (A) Flow plots showing the sorting gate of neutrophils and immature neutrophils for proteomics analysis. (B) Volcano plot showing the differentially expressed proteins of Ctrl_N vs. Ctrl_ImN, Ctrl_ImN vs. Elk1_ImN, Ctrl_N vs. Elk1_N groups. (C) Bar plots showing the top 10 differentially expressed KEGG signals of Ctrl_N vs. Ctrl_ImN, Ctrl_ImN vs. Elk1_ImN, Ctrl_N vs. Elk1_N groups. (D) GSEA analysis of the downregulated signals in wild type mice bone marrow derived immature neutrophils (Ctrl ImN) and Elane-Elk1 mice bone marrow derived immature neutrophils (Elk1_ImN) at the protein level (FDR < 0.25). (E) Venn diagrams showing the overlap of upregulated genes in Ctrl_ImN vs. Elk1_ImN, Ctrl_N vs. Elk1_N groups. (F) GO enrichment analysis of genes upregulated in immature neutrophils and mature neutrophils. (G) Heatmap showing the upregulated genes in both Elk1_ImN and Elk1_N compared to Ctrl_ImN and Ctrl_N. (H) Overall survival of AML patients with high (top 50%) and low (bottom 50%) expression of Lsp1, Trip4, Thbs1 and Ifitm3. N, neutrophils. ImN, immature neutrophil

that the expression of ELK1 in human AML cell lines has a positive correlation with many oncogenes such as KDM6A, KDM6B, KMT2A, KMT2B, MLLT3, MLLT11, MLLT10, IDH1, PML, DNMT3A, NRAS, KRAS and so on (Supplementary Fig. 1). However, these genes do not impede the differentiation and maturation of neutrophils but lead to clonal proliferation of cells. The cooperation of cell proliferation-related gene mutations and aberrant expression of lineage differentiation master regulators commonly occurs in AML [47]. The new function of ELK1 apart from other oncogenes in hematopoiesis and leukemogenesis still needs to be further elucidated due to the complex regulation of ELK1 in RNA splicing [22, 48], protein translocation [44] and self-limitation phosphorylation [23]. For example, opposite roles of L-ELK1 and S-ELK1 are observed in the differentiation of neuron cells [49], neutrophils [22] and erythrocytes [20]. Notably, S-ELK1 lacks DNA binding and phosphorylation domains. Thus, more accurate regulation of ELK1 at the RNA and protein levels needs to be applied to study the dynamic functions of ELK1 in hematopoiesis and leukemogenesis.

Our results demonstrate that inhibition of ELK1 activity suppressed the proliferation and promoted the differentiation of the OCI-AML3 cell line (which has an NPM1 mutation background). Additionally, ELK1 inhibition suppressed the proliferation of HL-60, Molm13 cell lines, but not that of NB4 or Kasumi-1 cell lines. Furthermore, we find that most downstream genes (4 out of 5) upregulated by ELK1 are downregulated by TDE in the OCI-AML3 cell line but not in other cell lines. Given the established role of ELK1 in neutrophil and erythrocyte lineage commitment and differentiation in early myeloid progenitors [20, 22] as well as the finding that obstruction of neutrophil lineage differentiation exacerbates the depletion of mature neutrophils and causes immune disorders in vivo, we propose that AML subtypes tend to be associated with disorders in the neutrophil or erythrocyte lineage-specifically, that inhibition of ELK1 can suppress the proliferation of leukemia cells in such subtypes. However, this hypothesis requires further experimental validation. Opposite roles of L-ELK1 and S-ELK1 have been reported in neural cell differentiation [49]. Our previous studies have shown L-ELK1 and S-ELK1 are differentially expressed in monocytes or monocyte progenitors versus neutrophils or neutrophil progenitors and play distinct roles in the lineage commitment and maturation of neutrophil and erythroid lineage cells-a phenomenon caused by different RNA splicing factors, such as SF3B1, SRSF11 [20, 22]. This finding indicates that RNA splicing dysregulation may lead to dysregulated expression of L-ELK1 and S-ELK1, thereby causing abnormal lineage differentiation. However, activation of RAS or ERK does not regulate the production of L-ELK1 and S-ELK1. ELK1 appears to play unique roles in the differentiation and maturation of neutrophil and erythroid lineage cells, and more precise regulatory mechanisms and functions of L-ELK1 and S-ELK1 need to be revealed in hematopoiesis and leukemogenesis. Thus, more specific and effective inhibitors or gene-editing approaches need to be developed for treating AML patients with elevated ELK1 expression.

Conclusions

We found that upregulation of Elk1 impedes the differentiation of neutrophils and accelerates the depletion of mature neutrophils under conditions of stress hematopoiesis, which promotes the development of myeloid neoplasm. Furthermore, we confirmed that inhibiting ELK1 can suppress the proliferation of leukemia cell lines and induce the differentiation of leukemic cells to generate mature $CD15^{+}CD66b^{+}$ neutrophils. All these results indicate that ELK1 might be an important therapy target for myeloid leukemia.

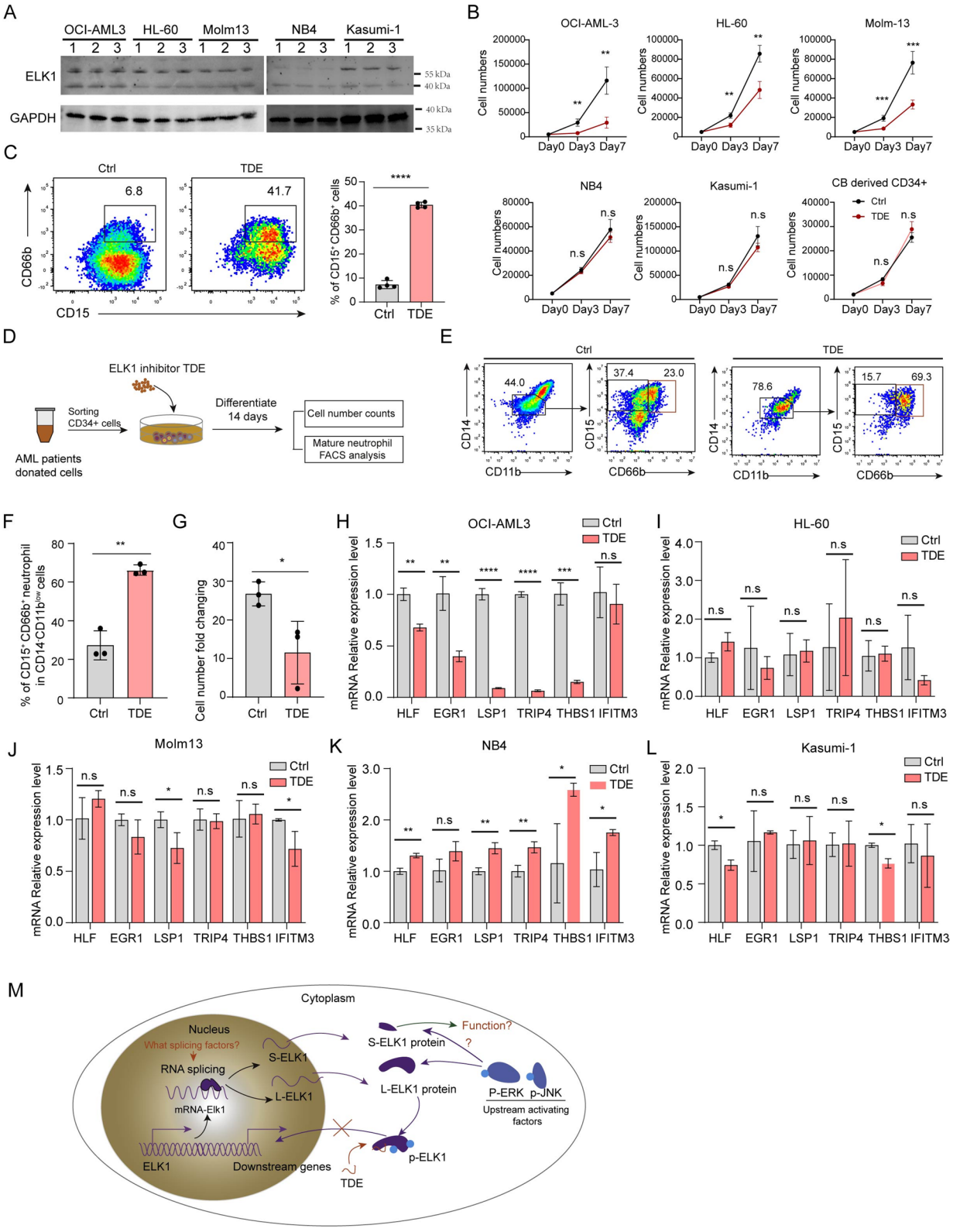

Fig. 7 (See legend on next page.)

(See figure on previous page.)

Fig. 7 Targeting ELK1 promotes AML cells differentiation. (A) Western blot images showing the expression level of ELK1 in OCI-AML3, HL-60, Molm-13, NB4 and Kasumi-1 human AML cell lines. (B) Line plots showing the changes in cell number of OCI-AML3, HL-60, Molm-13, NB4, Kasumi-1 and CD34 + HSPCs at day3 and day7 of treatment of TDE (1 μM). (C) Representative flow cytometry plots and statistical analysis showing the percentages of $CD66b^+CD15^+$ mature neutrophils derived from OCI-AML3 after 7 days of treatment with TDE. $N = 3$ replicates. n.s, no significance. $^{**}P < 0.01$, $^{***}P < 0.001$. (D) Schematic diagram of analyzing the impact of TDE in $CD34^+$ leukemia stem cells derived from human AML patients. (E-F) Representative flow cytometry plots and statistical analysis showing the percentages of $CD66b^+CD15^+$ mature neutrophils on primary $CD34^+$ leukemia stem cells from human AML patients after 14 days of treatment with TDE. $N = 3$ replicates. $^{**}P < 0.01$. (G) Relative cell proliferation fold change of human AML patients-derived $CD34^+$ leukemia stem cells after 14 days of treatment with TDE. $N = 3$ replicates. $^{*}P < 0.05$. (H-L) Bar plots showing the mRNA expression level of HLF, EGR1, LSP1, TRIP4, THBS1 and IFITM3 in OCI-AML3 (H), HL-60 (I), Molm-13 (J), NB4 (K) and Kasumi-1 (L) human AML cell lines after 3 days of treatment with TDE. Relative expression of the detected genes were calculated as 2^(-△△Ct), where △Ct = Ct(target gene)-Ct(housekeeping gene B2M); △△Ct=△Ct(Treated sample)- △Ct(Ctrl sample). $N = 3$–4 replicates; n.s, no significance; $^{*}P < 0.05$, $^{**}P < 0.01$, $^{***}P < 0.001$, $^{****}P < 0.0001$. (M) A schematic diagram illustrating the complex regulatory network of ELK1. The bar plots (F-L) are presented as the mean ± SD. An unpaired Student's t-test (two-tailed) was performed

Abbreviations

HSC	Hematopoietic stem cell
HSPC	Hematopoietic stem and progenitor cell
GMP	Granulocyte-monocyte progenitor
CMP	Common myeloid progenitor
MEP	Megakaryocyte-erythrocyte progenitor
SCF	Stem cell factor
IL-3	Interleukin-3
IL-6	Interleukin-6
TPO	Thrombopoietin
EPO	Erythropoietin
FLT3L	FMS-like tyrosine kinase-3 ligand
G-CSF	Granulocyte colony stimulating factor
GM-CSF	Granulocyte-macrophage colony stimulating factor
LSK	Lin (CD2, CD3, CD4, CD8, CD11b, B220, Ter19, Mac1)$^-$ $Sca1^+$ $ckit^+$
BM	Bone marrow
AML	Acute myeloid leukemia

Supplementary Information

The online version contains supplementary material available at https://doi.org/10.1186/s40164-025-00742-4.

Supplementary Material 1

Acknowledgements

We thank professor Yuhuan Zheng (Department of Hematology/Institute of Hematology, West China Hospital, Sichuan University) for providing HL-60, Molm-13, Yongping Zhang (Department of Hematology and Oncology, Children's Hospital of Soochow University) for providing the AML patients donated leukemia cells, Jiaxin Liu (J.X.L)(Institute of Blood Transfusion, Chinese Academy of Medical Sciences & Peking Union Medical College (CAMS & PUMC)) for funding support.

Author contributions

Yong Dong conceived, initialed, designed and analyzed all the data for this project. Yuhan He, Ya Zhou and Dexin Wen performed experiments. Rongqun Guo and Juan Du helped to collect and interpret the data. Yuhan He, Sizhou Huang and Yong Dong discussed and wrote this manuscript. Yong Dong and Ya Zhou provided funds for this research. All authors read and approved of the final manuscript. Yuhan He, Ya Zhou and DeXin Wen contributed equally to this work.

Funding

This research is supported by the National Key Research and Development Program of China (2023YFC3403800/2023YFC3403802 to D.Y), the National Natural Science Foundation of China (82470122 and 82200127 to D.Y), the Advanced Talents Training Program of Chengdu Medical College (CMC) (KYPY22-01 to D.Y), the CMC Excellent-talent program (2024yxGzn03 to D.Y), the National Natural Science Foundation of China (82470125 to Y.Z.) and the CAMS Initiatives for Innovative Medicine (2021-I2M-1-060 to J.X.L) .

Data availability

All the RNA-Seq data are deposited in NCBI's Gene Expression Omnibus (GEO) dataset with the accession number GSE299179. Other data supporting this study and materials are available from the corresponding author upon request.

Declarations

Ethics approval and consent to participate

Ethics approval and consent to participate. This research does not contain clinical experiments. All the animal experiments are performed at Chengdu Medical College. All animal experiments were approved by the Institutional Animal Care and Use Committee of Chengdu Medical College. The Approval Number is 2024-043.

Consent for publication

All the authors agree to publish the results of this study.

Competing interests

The authors declare no competing interests.

Author details

[1]Department of Immunology, School of Basic Medical Sciences, Chengdu Medical College, Xindu Road 783, Chengdu 610500, China
[2]Cell and Gene Therapy Center, Institute of Blood Transfusion, Chinese Academy of Medical Sciences & Peking Union Medical College (CAMS & PUMC), Chengdu, China
[3]Public Research Platform Management Center/ Translational Medical Center, The First Affiliated Hospital of Zhengzhou University, Zhengzhou, Henan, China
[4]Department of Hematology, The First Affiliated Hospital of Jinan University, Guangzhou, Guangdong, China
[5]Department of Anatomy and Histology and Embryology, School of Basic Medical Sciences, Chengdu Medical College, Chengdu, China

Received: 2 September 2025 / Accepted: 30 December 2025
Published online: 20 January 2026

References

1. Pollyea DA, et al. Acute myeloid Leukemia, version 3.2023, NCCN clinical practice guidelines in oncology. J Natl Compr Canc Netw. 2023;21(5):503–13.
2. Kutny MA, et al. Assessment of arsenic trioxide and All-trans retinoic acid for the treatment of pediatric acute promyelocytic leukemia: A report from the children's oncology group AAML1331 trial. JAMA Oncol. 2022;8(1):79–87.
3. Hanno, Hock et al. *Intrinsic Requirement for Zinc Finger Transcription Factor Gfi-1 in Neutrophil Differentiation.* immunity, 2003. 18: pp. 109–120.
4. Avellino R, et al. An autonomous CEBPA enhancer specific for myeloid-lineage priming and neutrophilic differentiation. Blood. 2016;127(24):2991–3003.
5. Pavithra, Shyamsunder, et al. Identification of a novel enhancer of CEBPE essential for granulocytic differentiation. Blood. 2019;133(23):2507–17.
6. Yáñez A, et al. IRF8 acts in lineage-committed rather than oligopotent progenitors to control neutrophil vs monocyte production. Blood. 2015;125(9):1452–9.
7. Li K, et al. CEBPE expression is an independent prognostic factor for acute myeloid leukemia. J Transl Med. 2019;17(1):188.
8. Hones JM, et al. GFI1 as a novel prognostic and therapeutic factor for AML/MDS. Leukemia. 2016;30(6):1237–45.

9. Georgi J-A, et al. Prognostic impact of CEBPA mutational subgroups in adult AML. Leukemia. 2024;38(2):281–90.
10. Zeng H, et al. Transcription factor Gfi1 regulates self-renewal and engraftment of hematopoietic stem cells. EMBO J. 2004;23(20):4116–25.
11. Avellino R, et al. Induced cell-autonomous neutropenia systemically perturbs hematopoiesis in Cebpa enhancer-null mice. Blood Adv. 2022;6(5):1406–19.
12. Serwas NK, et al. CEBPE-Mutant specific granule deficiency correlates with aberrant granule organization and substantial proteome alterations in neutrophils. Front Immunol. 2018;9:588.
13. Xue L, et al. NrasG12D oncoprotein inhibits apoptosis of preleukemic cells expressing Cbfβ-SMMHC via activation of MEK/ERK axis. Blood. 2014;124(3):426–36.
14. Carratt SA, et al. Mutant SETBP1 enhances NRAS-driven MAPK pathway activation to promote aggressive leukemia. Leukemia. 2021;35(12):3594–9.
15. Jay F, Dorsey JMC, Shrikant M, Mane, Wu J. *Regulation ofthe Erk2-Elk1 signaling pathway and megakaryocytic differentiation ofBcr-Abl K562 leukemic cells by Gab2.* blood, 2002.
16. Gao Y et al. Mechanical strain promotes skin fibrosis through LRG-1 induction mediated by ELK1 and ERK signalling. Commun Biology, 2019. 2(1).
17. Li K, et al. BCL6 is regulated by the MAPK/ELK1 axis and promotes KRAS-driven lung cancer. J Clin Invest. 2022;132(22):1–15.
18. Ma J, et al. BMP4 promotes oxaliplatin resistance by an induction of epithelial-mesenchymal transition via MEK1/ERK/ELK1 signaling6in6hepatocellular carcinoma. Cancer Lett. 2017;411:117–29.
19. Khalaf WF, et al. K-Ras is essential for normal fetal liver erythropoiesis. Blood. 2005;105(9):3538–41.
20. Zhang Y, et al. Small-molecule α-lipoic acid targets ELK1 to balance human neutrophil and erythrocyte differentiation. Volume 15. Stem Cell Research & Therapy; 2024. 1.
21. Behre G, et al. Ras signaling enhances the activity of C/EBPα to induce granulocytic differentiation by phosphorylation of Serine 248. J Biol Chem. 2002;277(29):26293–9.
22. Dong Y, et al. Dissecting the process of human neutrophil lineage determination by using alpha-lipoic acid inducing neutrophil deficiency model. Redox Biol. 2022;54:102392.
23. Anastasia Mylona F-XT, 2† C, Foster TM. Cheng,3 Francesc Miralles,1,4 Paul A. Bates,3 Philipp Selenko,2 Richard Treisman1‡, *Opposing effects of Elk-1 multisite phosphorylation shape its response to ERK activation.* Science, 2016. 354(6309): pp. 233–237.
24. Shen-Hsi Yang PS, Willingham N, Jeremy H.Lakey and, Andrew D, Sharrocks. The mechanism of phosphorylation-inducible activation of the ETS-domain transcription factor Elk-1. EMBO J. 1999;18(20):5666–74.
25. Dong Y et al. Synergy of NUP98-HOXA10 fusion gene and NrasG12D mutation preserves the stemness of hematopoietic stem cells on culture condition. Cells, 2019. 8(9).
26. Zhang M, et al. Transcription factor Hoxb5 reprograms B cells into functional T lymphocytes. Nat Immunol. 2018;19(3):279–90.
27. Tang F, et al. RNA-Seq analysis to capture the transcriptome landscape of a single cell. Nat Protoc. 2010;5(3):516–35.
28. Wang T, et al. Trim27 confers myeloid hematopoiesis competitiveness by up-regulating myeloid master genes. J Leukoc Biol. 2018;104(4):799–809.
29. Kishtagari A, Levine RL, Viny AD. Driver mutations in acute myeloid leukemia. Curr Opin Hematol. 2020;27(2):49–57.
30. Metzeler KH, et al. Spectrum and prognostic relevance of driver gene mutations in acute myeloid leukemia. Blood. 2016;128(5):686–98.
31. Kwok I et al. *Combinatorial Single-Cell Analyses of Granulocyte-Monocyte Progenitor Heterogeneity Reveals an Early Uni-potent Neutrophil Progenitor.* Immunity, 2020.
32. Cesari F, et al. Mice deficient for the Ets transcription factor Elk-1 show normal immune responses and mildly impaired neuronal gene activation. Mol Cell Biol. 2004;24(1):294–305.
33. Bernhard Lehnertz JC, MacRae T, Tomellini E, Corneau S, Mayotte N, Boivin I. Aurélie Durand, Deanne Gracias, guy Sauvageau, *HLF expression defines the human hematopoietic stem cell state*. Blood. 2021;138(25):2642–54.
34. Ramos-Mejia V, et al. HOXA9 promotes hematopoietic commitment of human embryonic stem cells. Blood. 2014;124(20):3065–75.
35. Yoshihara H, et al. Thrombopoietin/MPL signaling regulates hematopoietic stem cell quiescence and interaction with the osteoblastic niche. Cell Stem Cell. 2007;1(6):685–97.
36. Min IM, et al. The transcription factor EGR1 controls both the proliferation and localization of hematopoietic stem cells. Cell Stem Cell. 2008;2(4):380–91.
37. Kurtz KJ, et al. Murine models of acute myeloid leukemia. Front Oncol. 2022;12:854973.
38. Cesari F, et al. Elk-1 knock-out mice engineered by Flp recombinase-mediated cassette exchange. Genesis. 2004;38(2):87–92.
39. Li T et al. LSP1 promotes the progression of acute myelogenous leukemia by regulating KSR/ERK signaling pathway and cell migration. Hematology, 2024. 29(1).
40. Zhu L et al. THBS1 is a novel serum prognostic factors of acute myeloid leukemia. Front Oncol, 2020. 9.
41. Liu Y, et al. High IFITM3 expression predicts adverse prognosis in acute myeloid leukemia. Cancer Gene Ther. 2020;27(1–2):38–44.
42. Burgess MR, et al. Preclinical efficacy of MEK Inhibition in Nras-mutant AML. Blood. 2014;124(26):3947–55.
43. Apazoglou K, et al. Antidepressive effects of targeting ELK-1 signal transduction. Nat Med. 2018;24(5):591–7.
44. Lavaur J, et al. A TAT–DEF–Elk-1 peptide regulates the cytonuclear trafficking of Elk-1 and controls cytoskeleton dynamics. J Neurosci. 2007;27(52):14448–58.
45. Hu J, et al. Long-term efficacy and safety of all-trans retinoic acid/arsenic trioxide-based therapy in newly diagnosed acute promyelocytic leukemia. Proc Natl Acad Sci U S A. 2009;106(9):3342–7.
46. Lyubynska N et al. A MEK inhibitor abrogates myeloproliferative disease in Kras mutant mice. Sci Transl Med, 2011. 3(76).
47. Papaemmanuil E, et al. Genomic classification and prognosis in acute myeloid leukemia. N Engl J Med. 2016;374(23):2209–21.
48. Rahim G, et al. Alternative splicing within the elk-1 5′ untranslated region serves to modulate initiation events downstream of the highly conserved upstream open reading frame 2. Mol Cell Biol. 2023;32(9):1745–56.
49. Vanhoutte P, et al. Opposing roles of Elk-1 and its brain-specific isoform, short Elk-1, in nerve growth factor-induced PC12 differentiation. J Biol Chem. 2001;276(7):5189–96.

Publisher's note